MCB Accepts, published online ahead of print on 22 July 2013
Mol. Cell. Biol. doi:10.1128/MCB.00025-13

The yeast Snt2 protein coordinates the transcriptional response to hydrogen peroxide-mediated oxidative stress

RUNNING TITLE: Snt2 regulates transcription after oxidative stress

Lindsey A. Baker[1], Beatrix M. Ueberheide[2‡], Scott Dewell[3], Brian T. Chait[2], Deyou Zheng[4,5], and C. David Allis[#1]

[1]Laboratory of Chromatin Biology & Epigenetics, The Rockefeller University, NCew York, New York, 10065 USA

[2]Laboratory of Mass Spectrometry and Gaseous Ion Chemistry, The Rockefeller University, New York, NY, 10065, USA

[3]Genomics Resource Center, The Rockefeller University, New York, New York 10065 USA

[4]Departments of Neurology, Genetics, and Neuroscience, Albert Einstein College of Medicine, Bronx, New York, 10461 USA

[5]Departments of Neurology and Neuroscience, Albert Einstein College of Medicine, Bronx, New York, 10461 USA

[‡]present address: NYU School of Medicine, New York, NY 10016 USA

[#]corresponding author, email: alliscd@mail.rockefeller.edu, phone (212) 327-7839, fax (212)327-7849

Materials and Methods word count: 1,962

Introduction, Results, Discussion word count: 6,027

ABSTRACT

Regulation of gene expression in a vital part of the cellular stress response, yet the full set of proteins that orchestrate this regulation remains unknown. Snt2 is a yeast protein whose function has not been well characterized, that was recently shown to associate with Ecm5 and the Rpd3 deacetylase. Here, we confirm that Snt2, Ecm5, and Rpd3 physically associate. We then demonstrate that cells lacking Rpd3 or Snt2 are resistant to hydrogen peroxide (H_2O_2)-mediated oxidative stress, and use chromatin immunoprecipitation followed by high-throughput sequencing (ChIP-seq) to show that Snt2 and Ecm5 recruit Rpd3 to a small number of promoters and in response to H_2O_2, colocalize independent of Rpd3 to promoters of stress response genes. By integrating ChIP-seq and expression analysis, we identify target genes that require Snt2 for proper expression after H_2O_2. Finally, we show that cells lacking Snt2 are also resistant to nutrient stress imparted by the TOR pathway inhibitor rapamycin, and identify a common set of genes targeted by Snt2 and Ecm5 in response to both H_2O_2 and rapamycin. Our results establish a function for Snt2 in regulating transcription in response to oxidative stress, and suggest Snt2 may also function in multiple stress pathways.

INTRODUCTION

The ability of cells to respond to stressful conditions is crucial to survival and involves both the rapid activation of stress defense proteins to begin detoxifying or protecting against the stress and gene expression changes, which bolster the stress response but take longer to manifest. In the budding yeast, *Saccharomyces cerevisiae*, numerous types of stress, including heat shock, oxidative stress, and nitrogen starvation, promote similar changes in a core set of genes called the "Environmental Stress Response" or ESR (1, 2). As part of the ESR, genes involved in RNA processing, translation, and ribosomal biogenesis are repressed while genes involved in carbohydrate metabolism, protein folding, detoxification of reactive oxygen species (ROS), and maintaining redox balance are activated. These changes redirect energy away from basic metabolism towards stress detoxification and adaptation.

While the ESR is enacted similarly in response to diverse stresses, the levels and timing of gene expression changes vary depending on the type of stress, and distinct stresses promote additional changes in unique sets of genes (1). For example, while genes involved in ROS detoxification are all activated as part of the ESR, these genes are activated at higher levels when cells are exposed to oxidative stress through treatment with H_2O_2 (1). The stress-specific differences in the timing and extent of gene expression changes suggest that complex mechanisms regulate the ESR.

While numerous chromatin and transcriptional regulators have been linked to stress gene regulation (3-5), the full complement of proteins involved in this crucial function remains unknown. The yeast Snt2 protein was previously found to be enriched at promoter regions (6), suggesting that Snt2 may regulate transcription. In addition, Snt2 was recently reported to interact with Ecm5 and the Rpd3 deacetylase (7). Ecm5 was identified in a screen for cell wall

mutants (8), but like Snt2, contains protein domains expected to associate with chromatin (Fig. 1A). Rpd3 is a lysine deacetylase known to associate with two other well-characterized complexes, Rpd3(L) and Rpd3(S) (9-11). The Rpd3(L) complex has been reported to function in numerous pathways, and notably, has been linked to ESR regulation (12-16). However, the function of Snt2, either on its own or in association with Ecm5 and Rpd3, remains unclear.

Multiple lines of evidence point to a role for Snt2 in the oxidative stress response or possibly, in the ESR more generally. First, deletion of Snt2's reported interaction partner *ECM5* results in synthetic sickness when combined with deletion of *ASK10* (17), a gene originally identified as a high-copy enhancer of the Skn7 stress transcription factor that is involved in the oxidative stress response (18, 19). In addition, *snt2*Δ cells have increased phosphorylation of Slt2 (20), a mitogen activated protein kinase (MAPK) phosphorylated in response to oxidative and other stresses (21). Finally, an integrated pathway analysis based on published stress-induced transcription changes and Snt2 genomic localization data reported a link between Snt2 and the osmotic stress response (22).

We set out to determine whether Snt2 was involved in regulating the transcriptional response to oxidative stress. We first confirmed that Snt2 physically associated with Ecm5 and Rpd3, and found that cells lacking Snt2 or Rpd3 were resistant to H_2O_2-mediated oxidative stress. To better understand how Snt2 and Ecm5 might function during stress, we used ChIP-seq to map the genomic localizations of each protein before and 30 minutes after H_2O_2 treatment, and identified two categories of promoters targeted by Snt2 and Ecm5, promoters very highly enriched for Snt2 and Ecm5 regardless of stress, at which both proteins were required to recruit Rpd3, and promoters at which Snt2 and Ecm5 localized independently of Rpd3 in response to H_2O_2 stress. RNA-seq analysis identified target genes that required Snt2 was for proper

87 expression changes H_2O_2 stress, including genes involved in the ESR. Finally, the *snt2*Δ strain
88 was also resistant to nutrient stress imparted by the TOR pathway inhibitor rapamycin, and
89 rapamycin treatment enhanced Snt2 and Ecm5 localization to a subset of the H_2O_2 target
90 promoters. Our results identify a role for Snt2 in regulating transcription in response to oxidative
91 stress and further suggest Snt2 may have broad roles in stress gene regulation.
92
93

RESULTS

Snt2 physically associates with Ecm5 and the Rpd3 deacetylase

In order to better understand the function of Snt2, we first sought to confirm a previous report that Snt2 interacted with Ecm5 and Rpd3 (7). We tagged the C-terminus of Snt2 with a Protein A (PrA) tag (23) and affinity-purified Snt2-PrA and associated proteins from cryogenically-prepared yeast lysates (Fig. 1B). Liquid chromatography mass spectrometric (LC-MS) analysis identified both Ecm5 and Rpd3 in the Snt2-PrA purification and not in a control purification from an untagged strain (Table 2 and Dataset S1). To further confirm these associations, we repeated our affinity purifications using a strain in which Ecm5 was PrA-tagged. Consistent with the Snt2-PrA affinity purification, Snt2 and Rpd3 were both identified co-purifying with Ecm5-PrA (Fig. 1C and Dataset S1).

Rpd3 is known to associate with two well-characterized protein complexes, Rpd3(L) and Rpd3(S) (9, 10). With the exception of Rpd3, components of the Rpd3(L) and (S) complexes were not identified in Snt2- or Ecm5-PrA affinity purifications (Table 2 and Dataset S1), suggesting that Snt2 and Ecm5 associate with Rpd3 independently of Rpd3(L) and (S). We next performed an affinity purification with a PrA-tagged Rpd3 strain. LC-MS analysis of this purification identified 10 out of 12 and 5 out of 5 of the known Rpd3-interacting proteins from the Rpd3(L) and (S) complexes, respectively (Dataset S1). In addition, 3 Snt2 and 3 Ecm5 peptides were also identified (Dataset S1). To overcome potential suppression of signal for Snt2 and Ecm5 peptides by more abundant Rpd3-interacting proteins, a portion of the Rpd3-PrA purification was also resolved on an SDS-PAGE gel, and Coomassie-stained gel bands corresponding in size to Snt2 and Ecm5 were excised and analyzed by LC-MS, confirming the presence of Snt2 and Ecm5 peptides in the Rpd3-PrA purification (Dataset S1).

To further confirm these results, we generated a strain in which Ecm5 and Snt2 were tagged with 13 copies of the Myc epitope or with a GFP tag, respectively. Tagged Ecm5 was immunoprecipitated using a Myc antibody, and immunoblot analysis confirmed that Snt2-GFP and Rpd3 both co-precipitated with Ecm5-Myc (Fig. 1D). In contrast, Sin3, a component of the Rpd3(L) and (S) complexes did not co-precipitate with Ecm5-Myc (Fig. 1D). Taken together, our results confirm that Snt2, Ecm5, and Rpd3 physically associate in a form separable from Rpd3(L) and Rpd3(S).

Cells lacking Snt2 or Rpd3 are resistant to H_2O_2-induced oxidative stress

We next sought to determine the function of Snt2, either alone or in association with Ecm5 and Rpd3. A recent genetic screen found that deletion of *ECM5* resulted in synthetic sickness when combined with deletion of the *ASK10* gene (17), which encodes a protein involved in the oxidative stress response (18). Furthermore, cells lacking Snt2 have higher levels of phosphorylation of the stress MAPK Slt2 (20), and a bioinformatics study suggested that Snt2 might function to activate genes in response to stress (22). Rpd3 is known to regulate the response to numerous stresses, including oxidative stress, often as a part of the Rpd3(L) complex (12-15). Based on these data, we hypothesized that Snt2, Ecm5 and Rpd3 might function as an additional regulator of the oxidative stress response.

To test this hypothesis, we spotted serial dilutions of wild-type, *snt2*Δ, *ecm5*Δ, and *rpd3*Δ strains on untreated or H_2O_2-treated plates. While the strains all grew similarly on untreated plates (with the *rpd3*Δ strain having a slight growth defect), there was marked contrast in the growth of these strains on plates containing H_2O_2 (Fig. 2A). The wild-type and *ecm5*Δ strains showed strong H_2O_2 sensitivity. Consistent with the known role for Rpd3 in regulating the yeast

oxidative stress response as part of the Rpd3(L) complex, the *rpd3*Δ strain was resistant to H_2O_2. Strikingly, the *snt2*Δ strain was even more resistant to H_2O_2 than the *rpd3*Δ strain, showing similar levels of resistance to a strain lacking Gpr1, a glucose sensor whose deletion was reported to result in H_2O_2 resistance (24). Consistent with previous reports (25), a strain lacking the oxidative stress transcription factor Yap1 was sensitive to H_2O_2 (Fig. 2A). Separately-derived *snt2*Δ and *rpd3*Δ strains constructed on the BY4742 background also showed H_2O_2 resistance in this assay (data not shown).

We next determined whether *snt2*Δ and *rpd3*Δ strains also showed H_2O_2 resistance using a liquid survival CFU assay (26). When wild-type or *ecm5*Δ cells were treated with H_2O_2 at a final concentration of 0.4 mM for 4 hours, approximately 20% of cells survived (Fig. 2B). In contrast, the *rpd3*Δ strain had enhanced survival, with an average survival rate of 40.7%. Moreover, greater than 50% of *snt2*Δ cells survived H_2O_2 treatment, a statistically significant difference from wild-type levels, confirming that cells lacking Snt2 are resistant to oxidative stress.

The differing H_2O_2 sensitivities of the *snt2*Δ, *rpd3*Δ, and *ecm5*Δ mutants suggested that despite their physical association, these proteins might have distinct functions in the oxidative stress pathway. In order to better understand how these proteins function to regulate stress tolerance, we next determined the H_2O_2 resistance of double-deletion strains for these factors. Surprisingly, deletion of *ECM5* reversed the H_2O_2 resistance seen in the *snt2*Δ strain (Fig. 2C), suggesting that Ecm5 has a function in the oxidative stress response that is opposed to that of Snt2. Although the *snt2*Δ*rpd3*Δ double knockout possessed a modest growth defect similar to that of the *rpd3*Δ strain (as can be seen by the smaller size of the *snt2*Δ*rpd3*Δ colonies in Fig. 2C), the double knockout was more H_2O_2-resistant than the *rpd3*Δ strain alone, showing similar

levels of resistance to the *snt2*Δ strain. This result suggests that deletions of *RPD3* and *SNT2* promote stress resistance through different pathways, with the stress resistance of the *rpd3*Δ strain possibly relating to the known role of the Rpd3(L) complex in regulating the oxidative stress response. In agreement, strains lacking the Rpd3(L) complex members Sin3, Sap30, or Cti6 were also H_2O_2-resistant (Fig. 2D). Taken together, these results suggest that even though Snt2, Ecm5, and Rpd3 physically associate in cells Snt2 performs a function in the oxidative stress response distinct from those of Ecm5 or Rpd3.

Similar levels of Snt2, Ecm5, and Rpd3 associate with one another before and after H_2O_2 treatment

We next determined whether oxidative stress affected the associations between Snt2, Ecm5, and Rpd3. Immunoblot analysis of Ecm5-Myc, Snt2-GFP, and Rpd3 protein levels in Myc immunoprecipitations from *ECM5-MYC SNT2-GFP* or *SNT2-GFP* strains, did not reveal significant differences in the levels of Snt2-GFP and Rpd3 associating with Ecm5-Myc before and after H_2O_2 treatment (Fig. 3A). Similarly, when Rpd3 was immunoprecipitated from *ECM5-MYC SNT2-GFP* lysates, there were not differences in the levels of Snt2-GFP and Ecm5-Myc co-precipitating with Rpd3 before and after H_2O_2 stress (Fig. 3B, we note that while there was slightly more Ecm5-Myc and Snt2-GFP detected in the immunoprecipitation from the H_2O_2-treated cells, there was also more Rpd3 precipitated). Thus, H_2O_2 stress does not result in changes in the levels of Snt2, Ecm5, and Rpd3 physically associating.

In response to H_2O_2 stress, Snt2 and Ecm5 colocalize to gene promoters

To better understand how Snt2 and Ecm5 function in the oxidative stress response, we used ChIP-seq to map the genomic localizations of Myc-tagged Snt2 or Ecm5 both before and 30 minutes after H_2O_2 treatment. We chose to focus on Snt2 and Ecm5 to avoid having to disambiguate Rpd3 localization associated with Snt2 and Ecm5 from Rpd3 localization via the Rpd3(L) and (S) complexes. Consistent with their physical association, the Snt2 and Ecm5 ChIP profiles were strikingly similar (representative region shown in Fig. 4A). Both before and after H_2O_2 treatment, the majority of peaks of Snt2 enrichment overlapped with Ecm5 peaks by at least 200 bp (Fig. 4B). Scatterplots confirmed correlations between Snt2 and Ecm5 enrichment levels (Fig. 4C, Pearson's correlations = 0.895 and 0.917 for the 0 minute and 30 minute datasets, respectively).

We next analyzed the genomic distributions of Snt2 and Ecm5 peaks for enrichment at particular genetic features (Fig. 4D). Before treatment, 43% of peaks fell in promoter regions, while 23% fell within open reading frame (ORF) regions. Reads from an untagged control strain were also enriched in ORF peak regions (data not shown), suggesting that the ORF peaks may be an artifact reflecting the higher accessibility of transcribed chromatin rather than real sites of Snt2/Ecm5 enrichment, an effect which has been previously reported for ChIP experiments involving other proteins (27). We therefore chose to focus on peaks localized to promoter regions for further study. Strikingly, 30 minutes after H_2O_2 treatment, Snt2 and Ecm5 underwent dramatic localization changes, with many regions showing new or enhanced localization of Snt2 and Ecm5 (Fig. 4A). After H_2O_2 treatment, 74% of peaks were in promoters (Fig. 4D). Alignments of Snt2 and Ecm5 ChIP-seq reads around the transcription start sites (TSSs) of all genes revealed Snt2 and Ecm5 enrichment approximately 250 bp upstream of the TSS in H_2O_2-

209 treated cells (Fig. 4E, dark purple line). In addition, there were 817 peaks of Snt2 and Ecm5
210 enrichment identified after treatment, compared to only 315 peaks present before (Fig. 4B). For
211 both Snt2 and Ecm5, the majority of peaks called in untreated samples were also present after
212 H_2O_2 treatment (Fig. 4F).

213 In order to compare between different ChIP-seq datasets, we generated a list of all peaks
214 of both Snt2 and Ecm5, identified before or after stress, and calculated Snt2 or Ecm5 enrichment
215 at each region before and after stress (see Methods). When all peaks were considered together,
216 enrichment of Snt2 and Ecm5 was significantly higher after treatment compared to before
217 treatment, consistent with the many new peaks identified in treated cells (Fig. 4G). Similarly,
218 scatterplots showing Snt2 or Ecm5 enrichment at all peak regions before treatment compared to
219 enrichment after treatment, show that the majority of peaks had enrichment scores at least 1.5-
220 fold higher after H_2O_2 treatment compared to enrichment before treatment (Fig. 4H, note that
221 purple points outnumber gray and orange points).

222 To look for motifs in Snt2/Ecm5 target sites, we used the de novo motif finder Meme
223 (28). The 100 bp centered around each peak's summit (determined by MACS) was used for this
224 analysis. While no motif was significantly enriched when all peaks were analyzed together, when
225 we used 20 peaks with the highest Snt2/Ecm5 enrichment levels for this analysis, a motif
226 containing [AG][CT]GGCGCTA[CTA]CA was strongly enriched (Fig. 4I, E-value $1.3X10^{-7}$), in
227 agreement with an Snt2-binding motif identified in a previous Snt2 ChIP-chip study,
228 [CT]GGCGCTA[CT]CA (6). We next analyzed the peaks where Snt2 and Ecm5 levels were at
229 least 1.5-fold higher after H_2O_2 treatment (purple points in Fig. 4H). A second motif,
230 CCG[CT]GGA, was identified among these H_2O_2-enriched Snt2/Ecm5 peaks (Fig. 4I, right, E-
231 value $1X10^{-3}$). This motif is similar to the previously published motifs of the Pdr1 and Pdr3

232 transcription factors (CCGCGGA) (29), which regulate cellular transport genes (30).
233 Collectively, these results show that H_2O_2 treatment stimulates Snt2 and Ecm5 to colocalized to
234 promoters, and identify Pdr1 and Prd3 as potential factors that may cooperate with Snt2 and
235 Ecm5.
236
237 **After H_2O_2 treatment, Snt2 and Ecm5 localize to promoters of genes involved in oxidative**
238 **stress and cellular metabolism**
239 We next sought to determine which categories of genes were targeted by Snt2 and Ecm5
240 as a result of oxidative stress. As described above, we identified peaks in which Snt2/Ecm5
241 enrichment increased, decreased, or did not change after H_2O_2 treatment (purple, orange, and
242 gray points, respectively, in Fig. 4H), and analyzed each set of target genes using Gene Ontology
243 (GO) analysis (31). Genes whose promoters had decreased levels of Snt2 and Ecm5 after H_2O_2
244 stress were involved in protein metabolism (ribosome and translation) (Fig. 4J). Genes whose
245 promoters had similar levels of Snt2 and Ecm5 before and after treatment also functioned in
246 protein metabolism, as well as in carbohydrate metabolism (gluconeogenesis and glycolysis and
247 transposition, Fig. 4J). Thus, in unstressed cells, Snt2 and Ecm5 target sugar and protein
248 metabolism genes.
249 Genes where Snt2 and Ecm5 levels increased after H_2O_2 treatment had functions amino
250 acid, steroid, and alcohol metabolism (Fig. 4J). For example, after H_2O_2 treatment Snt2 and
251 Ecm5 were enriched at the promoters of the *BAT2* amino acid metabolism gene and the sterol
252 metabolism genes *ERG3* and *ERG6*, which help synthesize the cell wall component ergosterol
253 (Fig. 5A). While the cell wall category was not identified by GO analysis, we found additional
254 cell wall targeted by Snt2 and Ecm5 in response to H_2O_2 treatment, including the cell wall

glucanase *SCW10* and the glucan synthase *FKS3* (Fig. 5A). Ecm5 was originally identified in a screen for mutants with cell wall defects (8), and these results suggest a possible connection between Ecm5 function and cell wall maintenance. In response to stress, Snt2 and Ecm5 were also enriched at cellular transport genes (Fig. 4J) including the *FUI1* uridine permease (Fig 5A), consistent with the enrichment of a motif similar to that of the Pdr1 and Pdr3 transport gene regulators among Snt2/Ecm5 target sites. Notably, ergosterol biosynthesis, amino acid metabolism, and cellular transport genes are all categories regulated as part of the ESR (1), showing that in response to stress Snt2 and Ecm5 target ESR genes.

Consistent with genetic evidence linking Snt2 to oxidative stress regulation, genes involved in redox reactions and the oxidative stress response also had increased levels of Snt2 and Ecm5 after treatment (Fig. 4J). These included *CYC1*, which encodes the cytochrome *c* component of the mitochondrial electron transport chain, and *SUE1*, which encodes a protein that degrades unstable cytochrome *c* (Fig. 5A). The incomplete reduction of oxygen in the electron transport chain is one of the main endogenous sources of ROS in cells (32), and the association of Snt2 and Ecm5 with promoters of genes involved in cytochrome *c* biology further links these proteins to oxidative stress. In addition, after H_2O_2 treatment, Snt2 and Ecm5 were enriched in the promoters of the genes encoding the oxidative stress transcription factors, Yap1 and Cin5 (also known as Yap4) which are activated by oxidative stress (33, 34), the catalase Ctt1 and the superoxide dismutase Sod1, which have detoxify ROS (35), as well as the membrane proteins Hsp30 and Hsp12, which are induced in response to oxidative stress (36, 37) (Fig. 5A and data not shown). Increased Snt2 and Ecm5 localization to many of these promoters in response to H_2O_2 treatment was confirmed by ChIP-qPCR (Fig. 5B and data not shown).

A small number of promoters were very highly enriched for Snt2 and Ecm5

ChIP-seq analysis identified a small set of promoters very highly enriched for Snt2 and Ecm5 both before and after H_2O_2 treatment: while most peaks of Snt2 and Ecm5 enrichment had peak heights between 70 and 150 (representing the number of reads in the peak summit scaled by 1,000,000/total number of reads in that ChIP-seq experiment), we identified 10 "super-enriched" Snt2 and Ecm5 peaks in the promoters of 14 genes, with peak heights over 500 in both untreated and treated cells (Table 3). For example, Snt2/Ecm5 peaks at the promoters of *CYC3/CDC19*, *BNR1/POT1*, and *MSN1* were more than ten-fold more enriched than the peaks described in the previous section (compare bracketed scale bars in Fig. 6A with those in Fig. 5A). Independent ChIP-qPCR experiments recapitulated the high levels of Snt2 and Ecm5 enrichment found at these promoters (Fig. 6B), showing that these high enrichment levels are not merely sequencing artifacts.

While the only significant GO association found for the 14 super-enriched target genes was polysaccharide catabolism ($p= 2.7x10^{-5}$), likely due to the small number of genes, almost all of the genes had functions connected to the ESR (Table 3), including genes involved in carbohydrate metabolism (*GDB1*, *CDC19*, *PGU1*), fatty acid metabolism (*POT1*), ribosome biogenesis (*IPI3*), translation (*STM1*), amino acid transport (*CUP9*), redox reactions (*YNL181W, CYC3*), and general stress response (*SSA3*, *CUR1*, *MSN1*). The high levels of Snt2 and Ecm5 at super-enriched promoters may reflect high occupancy of these regions in all cells, or alternatively, a high proportion of cells in the culture that have Snt2 and Ecm5 occupied at these sites.

Snt2 and Ecm5 are required for Rpd3 recruitment to super-enriched promoters, but not for recruitment of the Rpd3(L) complex member Sds3

Because Rpd3 physically associated with Snt2 and Ecm5, we next determined whether Rpd3 also associated at Snt2/Ecm5 targets, and if so, in an Snt2- or Ecm5-dependent manner. Deletion of *ECM5* or *SNT2* from a Myc-tagged Rpd3 strain did not alter global levels of Rpd3-Myc before or after H_2O_2 treatment (Fig. 6C). By ChIP-qPCR, Myc-tagged Rpd3 was enriched at all Snt2/Ecm5 target promoters assayed, both before (data not shown) and after (Fig. 6D) treatment. Surprisingly, deletion of *SNT2* or *ECM5* abrogated Rpd3-Myc enrichment at Snt2/Ecm5 super-enriched promoters, but not at promoters where Snt2/Ecm5 were enriched after H_2O_2 treatment (Fig. 6D). Thus, there are at least two classes of Snt2/Ecm5 targets, those at which Snt2 and Ecm5 localize at high levels regardless of stress and recruit Rpd3, and those at which Snt2 and Ecm5 associate in response to H_2O_2 treatment, independently of Rpd3.

Because Rpd3 recruitment can also occur through association with the Rpd3(L) complex, and Rpd3(L) function has been linked to the yeast stress response (11-16), we sought additional confirmation that the Snt2- and Ecm5-dependent association of Rpd3 with super-enriched promoters occurred independently of the Rpd3(L) complex. We Myc-tagged the Rpd3(L) subunit Sds3, and used ChIP-qPCR to analyze Sds3-Myc association with Snt2/Ecm5 target promoters in the presence or absence of Snt2. Deletion of *SNT2* did not affect Sds3-Myc protein levels before or after H_2O_2 treatment (Fig. 6C). Sds3-Myc was not enriched above background levels at the *MSN1* or *IPI3/YNL181W* Snt2/Ecm5 super-enriched promoters (Fig. 6E), suggesting that at these targets, Snt2, Ecm5, and Rpd3 function independently from the Rpd3(L) complex. Sds3-Myc was modestly enriched at the super-enriched *CYC3*/*CDC19* promoter. However, Sds3-Myc

enrichment to these promoters and to the *EXG1* promoter, an H_2O_2-enriched Snt2/Ecm5 target, was not decreased when *SNT2* was deleted, showing that Snt2 and Ecm5 do not recruit Rpd3(L) to target promoters (Fig. 6E).

Snt2, but not Ecm5, is required for proper expression of ChIP target genes

Having shown that Snt2 and Ecm5 localize to ESR genes after H_2O_2 treatment, we next sought to determine whether Snt2 or Ecm5 regulated target gene expression. We performed RNA-sequencing (RNA-seq) analysis of wild-type, *snt2*Δ, or *ecm5*Δ strains before or 30 minutes after H_2O_2 treatment. The RNA-seq was performed in biological triplicate, and expression levels of many Snt2 and Ecm5 target genes were confirmed by qPCR analysis (data not shown). In wild-type cells, 3,127 genes significantly changed expression in response to H_2O_2 treatment (significance determined by the CuffDiff program). A previous microarray study reported 1,294 genes up- or down-regulated at least 2-fold in wild-type cells 30 minutes after treatment with 0.32 mM H_2O_2 (1). The larger number of genes identified in our study may reflect the higher sensitivity of the RNA-seq technique to identify transcription changes (CuffDiff can call fold differences below 2-fold significant if there are enough reads for the model to statistically call a difference), or possibly differences in the concentrations of H_2O_2 used in the two studies (0.4 mM in ours, compared to 0.32 mM in the previous study). Importantly, 1,030 of the 1,294 genes (80%) identified in the previous study were also up- or down-regulated in response to H_2O_2 treatment in our study ($p < 3x10^{-15}$ by hypergeometric test), confirming that the H_2O_2 triggered similar expression changes to those previously reported.

As expected, both before and after treatment, *ECM5* and *SNT2* were the genes most down-regulated in the *ecm5*Δ and *snt2*Δ strains, respectively. Deletion of *ECM5* had minimal

effects on gene expression: before treatment, only 33 genes differed in expression from wild-type levels, and only 7 genes differed from wild-type levels after treatment (Fig. 7A). In contrast, in the *snt2*Δ strain, 38 genes were down-regulated and 134 genes up-regulated relative to wild-type levels before H_2O_2 treatment, and 262 and 475 genes were down- and up-regulated, respectively, relative to wild-type levels after treatment (Fig. 7A). Few genes showed expression changes in both the *snt2*Δ and *ecm5*Δ strains. Notably, two cell wall mannoprotein genes, *FIT1* and *DAN1*, showed opposite expression changes in the two strains (Fig. 7B). These results again link Snt2 and Ecm5 function to cell wall regulation and are consistent with Snt2 and Ecm5 having opposing functions.

Like the genes targeted by Snt2 and Ecm5 in response to H_2O_2, the genes up- or down-regulated in the *snt2*Δ strain functioned in stress and metabolism pathways. Before H_2O_2 treatment, GO analysis identified genes involved in acetyl-CoA metabolism, NAD metabolism, oxidation-reduction processes, and the tricarboxylic acid cycle enriched among genes whose expression changed in the *snt2*Δ strain (p values: $8.8x10^{-7}$, $5.5x10^{-5}$, $1.3x10^{-6}$, and $5.8\ x10^{-8}$, respectively). After H_2O_2 treatment, genes up-regulated in the *snt2*Δ strain functioned in protein synthesis, rRNA processing, and hexose transport, while genes down-regulated functioned in translation, amino acid metabolism, ROS metabolism, and response to ROS (Fig. 7C), further linking Snt2 to oxidative stress and metabolism regulation.

By integrating our RNA-seq and ChIP-seq analyses, we identified 403 of the 1205 H_2O_2-enriched Snt2/Ecm5 target genes were up- or down-regulated at least 1.5-fold in the *snt2*Δ strain after treatment. Of those, 309 genes also changed expression in wild-type cells in response to H_2O_2 treatment (Fig. 7D), demonstrating considerable overlap between target genes directly regulated by Snt2 and target genes regulated through the oxidative stress response. Notably,

370 many of the Snt2 and Ecm5 targets involved in the oxidative stress response or in cytochrome *c*
371 regulation described above had altered expression levels in the *snt2*Δ strain after treatment (Fig.
372 7E). Taken together, these results show that H_2O_2 treatment prompts Snt2 to target and regulate
373 stress response genes.

374 When the 309 target genes regulated by Snt2 were clustered on their expression profiles,
375 4 clusters could be distinguished, encompassing genes whose expression increased (clusters 1
376 and 2) or decreased (clusters 3 and 4) in wild-type cells after H_2O_2 treatment, and genes whose
377 expression levels in the *snt2*Δ strain after treatment were higher (clusters 1 and3) or lower
378 (clusters 2 and 4) than wild-type expression levels (Fig. 7F). While a regulatory trend was not
379 readily observed when all 309 genes were considered together (Fig. 7G, left panel), distinct
380 patterns did emerge within specific categories of genes. For instance, all but one of the 24
381 translation genes in this set were down-regulated in the *snt2*Δ strain after treatment. In contrast,
382 38 of the 48 plasma membrane genes in this set were up-regulated in the absence of Snt2, as
383 were all 20 of the lipid metabolism genes, including the ergosterol metabolism genes.

384 Our expression results suggest that Snt2 functions to both promote and repress gene
385 expression, depending on the target. A possible mechanism through which this might occur may
386 be through Snt2-mediated stabilization of unique sets of transcriptional regulators at different
387 genes. As mentioned above, a subset of H_2O_2-enriched Snt2/Ecm5 target promoters contained a
388 motif similar to the motif of the Pdr1 and Pdr3 transcriptional regulators. To search for other
389 transcription factors that might cooperate with Snt2, we used the YEASTRACT program (38) to
390 search for factors with binding sites in the 309 Snt2-regulated target genes that changed
391 expression in wild-type cells in response to stress (Fig. 7H), and found that 205 of the 309 genes
392 are targets of the Ste12 transcription factor, which is activated downstream of the Fus3 and Kss1

mating and filamentous grown MAPK pathways, that is also activated by nutrient stress (39). In addition, 138 of the 309 genes were targets of Rap1, which functions as both a transcriptional activator and repressor depending on the target (40), and regulates ribosomal biogenesis genes (41). Thus, Ste12 and Rap1 may be two additional factors that potentially cooperate with Snt2 to regulate gene expression.

Treatment with the TOR pathway inhibitor rapamycin promotes Snt2 and Ecm5 localization to many of the same genes as H_2O_2 treatment

The genes regulated by Snt2 and targeted by Snt2 and Ecm5 after H_2O_2 treatment had numerous functions linked to stress response, including genes involved in metabolism and nutrient transport. We therefore hypothesized that rather than functioning solely in the oxidative stress response, Snt2 might function more broadly to regulate stress and metabolism. To test this, we interrogated the growth of the *snt2*Δ strain in the presence of rapamycin, a TOR pathway inhibitor which mimics nitrogen starvation (42). In dilution spotting assays, *snt2*Δ cells were resistant to rapamycin (Fig. 8A; the less nutrient-rich SD CSM media was chosen for these assays to ensure that the high levels of nutrients in YPD media did not compensate for a nutrient stress phenotype).

We used ChIP-seq to map Snt2 and Ecm5 localization in cells treated for 30 minutes with rapamycin or with DMSO as a control. Similar to H_2O_2 treatment, rapamycin treatment prompted increased Snt2 and Ecm5 association at multiple loci (marked with arrows in Fig. 8B). Of the 155 Snt2/Ecm5 peaks where Snt2 and Ecm5 levels increased at least 1.5-fold in response to rapamycin treatment, 116 were also regions where Snt2/Ecm5 levels increased after H_2O_2 treatment (Fig. 8C). For example, both H_2O_2 and rapamycin treatment prompted Snt2 and Ecm5

enrichment at the promoters of the *FUI1* uridine permease and *BAT2* amino acid aminotransferase genes (Fig. 8D). These results suggest that rather than being a unique regulator of oxidative stress, Snt2 regulate stress and metabolism more broadly.

DISCUSSION

All cells must balance allocation of energy to growth with allocation to stress defense mechanisms, and when exposed to stress, must rapidly shift investment to the latter. In yeast, this shift involves regulation of a common set of genes called the ESR (1, 2). However, the mechanisms through which these genes are regulated are not fully understood. Here, we have shown that Snt2 physically associates with Ecm5 and the Rpd3 deacetylase, and integrated phenotypic, ChIP-seq, and RNA-seq analyses to uncover an Rpd3-independent role for Snt2 in regulating genes in response to oxidative stress. While a previous study mapped Snt2 localization using ChIP-chip (6), to our knowledge, ours is the first study to map Snt2 using high-throughput sequencing, and more importantly, the first to examine the localization changes of either Snt2 or Ecm5 in response to stress.

Consistent with a previous report (7), our LC-MS analysis of affinity purifications from PrA-tagged Snt2, Ecm5, and Rpd3 cell lysates confirmed associations between these three proteins (Fig. 1, Table 2, Dataset S1). While Rpd3 is known to associate with two other complexes (9, 10), we did not identify subunits of either complex associating with Snt2 or Ecm5 (Fig. 1D, Table2, Dataset S1), suggesting that Snt2, Ecm5, and Rpd3 comprise a third Rpd3 complex.

Strikingly, both the *snt2*Δ and *rpd3*Δ strains were resistant to H_2O_2-mediated oxidative stress (Fig. 2A and B), leading us to initially hypothesize that Snt2, Ecm5, and Rpd3 functioned together in the oxidative stress response. We used ChIP-seq to identify regions where Snt2 and Ecm5 were localized before and 30 minutes after H_2O_2 treatment (Fig. 4) and surprisingly, identified at least two distinct types of Snt2/Ecm5 targets: a small number of promoter regions at which Snt2 and Ecm5 are required for Rpd3 localization (Fig. 6), and a much larger set of

444 promoters where Snt2 and Ecm5 localize independently of Rpd3 in response to H_2O_2 treatment
445 (Fig. 5).

446 In the first set of promoters, high levels of Snt2 and Ecm5 were detected in both
447 untreated and H_2O_2-treated cells (Fig. 6 A and B, Table 3). Rpd3 was enriched at these
448 promoters, and Snt2 and Ecm5 were required for Rpd3 enrichment (Fig. 6D and data not shown).
449 Consistent with our inability to detect Rpd3(L) subunits associating with Snt2 and Rpd3, deletion
450 of *SNT2* did not affect the localization of the Rpd3(L) complex member Sds3 (Fig. 6E), further
451 supporting the idea that Snt2, Ecm5, and Rpd3 function as a distinct complex. While many of
452 super-enriched promoters had functions linked to stress response, Snt2, Ecm5, and Rpd3
453 associated with these regions before and after H_2O_2 treatment. Furthermore, we did not detect
454 altered levels of Snt2-GFP, Ecm5-Myc, and Rpd3 associating with one another after H_2O_2
455 treatment (Fig. 3), suggesting that Snt2, Ecm5, and Rpd3 may have a stress-independent function
456 at these promoters. Surprisingly, while deletion of *SNT2* or *ECM5* decreased Rpd3 levels at these
457 promoters, we did not detect changes in histone H3 acetyl levels in these regions by ChIP-qPCR
458 (data not shown). Rpd3 may be recruited to these regions to deacetylate other histone substrates
459 or nonhistone proteins. Alternatively, association of Rpd3 with Snt2 and Ecm5 may inactivate it.
460 Consistent with the latter hypothesis, in *Drosophila*, association of Rpd3 with a complex
461 containing the Ecm5-homolog Lid was reported to inhibit deactetylase activity (43).

462 We identified a second set of promoters where levels of Snt2 and Ecm5 increased after
463 H_2O_2 stress (Fig. 4H and Fig. 5). While Rpd3 was enriched at these promoters by ChIP-qPCR,
464 deletion of *SNT2* or *ECM5* did not affect Rpd3 association (Fig. 6D), suggesting that other
465 proteins recruit Rpd3 to these targets. The Rpd3(L) complex regulates genes in response to
466 diverse stresses (13-16), including oxidative stress (12), and may recruit Rpd3 to these regions.

RNA-seq analysis identified 309 H_2O_2–enriched target genes that changed expression in wild-type cells in response to H_2O_2 and were either up- or down-regulated when *SNT2* was deleted (Fig. 7D), many of which function in oxidative stress response or oxidative metabolism (Fig. 7E).

While initially surprising that Snt2 might function as both an activator and a repressor, a number of other yeast transcriptional regulators, including Hap1 and Rap1, have been reported to have dual roles in transcription (40, 44, 45). The methods through which these proteins exert such opposing effects remain to be elucidated, but may involve the cooperation with unique factors at different promoters. A subset of the H_2O_2-enriched promoters contained a motif similar to the known Pdr1/Pdr3 motif (Fig. 4I), while many of Snt2/Ecm5 target genes regulated by Snt2 are also known to be targeted by Ste12 and Rap1 (Fig. 7H), suggesting that Pdr3, Pdr1, Ste12, and Rap1 may cooperate with Snt2 to regulate different gene sets.

Surprisingly, despite the physical association and genomic colocalization of Snt2 and Ecm5, our genetic data uncovered independent functions for these proteins in the response to H_2O_2 stress. The *ecm5*Δ strain was not resistant to oxidative stress like the *snt2*Δ strain (Fig. 2A and B) and had few gene expression changes (Fig. 7A), but deletion of *ECM5* from the *snt2Δ* strain reversed the H_2O_2 resistance of this strain (Fig. 2C), suggesting that Ecm5 has a function that is opposed to that of Snt2. In support, the synthetic sickness of the *ecm5*Δ*ask10*Δ double mutant (17), suggest Ecm5 function promoters oxidative stress tolerance, while Snt2 function ultimately decreases tolerance.

Because Snt2 and Ecm5 localized to genes that function in multiple pathways linked to the ESR, and not just to oxidative stress response genes, we hypothesized that rather than regulating only the oxidative stress pathway, Snt2 regulate stress pathways more broadly. In

support, the *snt2*Δ strain was resistant to rapamycin (Fig. 8A), and rapamycin treatment promoted Snt2 and Ecm5 association with a subset of the H_2O_2 target promoters (Fig. 8C and D). A recent study reported that *snt2*Δ strain was sensitive to histone over-expression (46). While the authors of that study propose that Snt2 functions in histone degradation, their results could also be explained if altered stress regulation in *snt2*Δ cells renders them more sensitive to the stress of histone over-expression.

The mechanism through which Snt2 and Ecm5 localization is regulated remains an exciting question, and could involve stress-specific protein associations, post-translational modifications, or regulation of subcellular distribution. Along these lines, our LC-MS analysis identified a phosphorylation site on serine 641 of Snt2 (Table 2). However, mutation of this serine to alanine or glutamate did not prevent ectopic Snt2 from rescuing the *snt2*Δ phenotype (data not shown), suggesting this residue is not required for stress-mediated Snt2 regulation. Of note, a recent protein localization study reported that Ecm5 localized to the nucleus, while Snt2 localized to both the cytoplasm and the nucleus and accumulated in the nucleus after nitrogen starvation (47). While this study did not find a change in Snt2 localization after H_2O_2 stress, we note that a higher concentration of H_2O_2 was used than in our study, possibly activating different stress pathways. Future studies aimed at providing insights into the mechanisms of Snt2 and Ecm5 regulation will be of considerable interest.

MATERIALS AND METHODS

Strains, growth conditions, and growth assays

All *S. cerevisiae* strains used in this work (Table 1) were derived from the S288C background strain and are isogenic with BY4741. Where noted, deletion strains were obtained from OpenBiosystems. Otherwise, strains were generated using standard genetic methods (48). Deletion strains were constructed by replacing the gene of interest with a PCR-amplified *KanMX4* or *HygMX4* marker through homologous recombination. Tagged strains were created by targeting PCR-amplified PrA, GFP, or 13Myc tags to the 5' ends of genes of interest, as previously described (23, 48). All strains were confirmed by PCR. Except where otherwise indicated, cells were grown in standard YPD media (1% yeast extract, 1% peptone, and 2% glucose). For rapamycin experiments, cultures were grown in synthetic defined media supplemented with complete supplement mixture (SD CSM, CSM from MP Biomedicals).

For plate spotting assays, saturated overnight cultures of each strain were diluted in YPD (for H_2O_2 plate assays) or SD CSM (for rapamycin plate assays) and grown 5-6 hours to mid-log phase (OD600=0.6). Strains were then diluted to $5x10^6$ cells/mL and used to make five-fold serial dilutions. 4 uL of each dilution were spotted onto plates supplemented as indicated in figure legends. Plates were poured no more than 20 hours prior to spotting. H_2O_2 and rapamycin plate assays were imaged after 2 and 3 days, respectively. Survival assays were performed as previously described (26), except that survival was determined after treatment with 0.4 mM H_2O_2 for 4 hours.

Affinity purification of Snt2, Ecm5, and Rpd3

BY4741, Snt2-PrA, Ecm5-PrA or Rpd3-PrA cultures were prepared for lysis and lysed under cryogenic conditions using a Retsch PM 100 planetary ball mill as described previously (49). 20g of each lysate was resuspended in 100 mL Lysis Buffer [20 mM HEPES pH 7.4, 2 mM MgCl, 300 mM NaCl, 0.1% Triton X-100, 0.1% Tween-20, 110 mM potassium acetate, 0.1 mg/mL PMSF, 2 ug/mL pepstatin, 0.5% protease inhibitor cocktail for fungal and yeast cells (Sigma)], homogenized for 10 seconds with a Polytron homogenizer, incubated for 10 minutes with 600 units of recombinant DNaseI (Roche), and clarified by centrifugation. Clarified lysates were mixed with equilibrated Dynabeads (Invitrogen) that had been conjugated with rabbit IgG as described previously (50). The rest of the purification was performed as described previously (51).

Mass spectrometric analysis of affinity purifications

For Snt2-PrA, Rpd3-PrA, and control purifications, elutions were concentrated to dryness using a Speedvac. Elutions were resuspended in 100 mM ammonium bicarbonate, reduced with 20 mM DTT for 1 hour at 57^{o}C, and alkylated with 45 mM iodoacetamide for 45 min in the dark at room temperature. Samples were digested with sequencing-grade modified trypsin (Promega) for 8 hours at 37^{o}C , and the digestion was stopped by acidifying the solution with glacial acetic acid. The solution was pressure loaded onto self-packed pre columns (360x75 um), rinsed with 0.5% acetic acid to remove salt and butt-connected to a nano-HPLC column with integrated 15 um emitter (360 x 75 um PicoTip emitter, New Objective) packed with 6 cm of 5 um C18 beads (YMC ODS AQ). The peptides were eluted with a linear gradient of 0-40%B in 50 min and 40-100%B in 70 min (A = 0.1M acetic acid, B = 70% acetonitrile in 0.1M acetic acid) using an

Agilent 1100 binary HPLC and analyzed on a Finnigan LTQ-XL mass spectrometer (Thermo Fisher) equipped with a nano-HPLC microelectrospray ionization source. The mass spectrometer was operated in a data-dependent mode where one full scan mass spectrum was followed by 10 collision activated dissociation (CAD) mass spectra of the 10 most abundant ions. The fragmented ions were set on an exclusion list for 40 s and the cycle repeated throughout the data acquisition. The resulting spectra were searched against the *Saccharomyces cerevisiae* database using the search algorithm X! Tandem (52). Proteins that have been previously reported to be contaminants of PrA affinity purifications (7, 53), were identified in a control purification from an untagged cell lysate, or are known to be highly abundant in yeast cells (54) were assumed to be contaminants.

For the Ecm5-PrA purification, elutions were reduced and alkylated as described above, immediately separated by SDS-PAGE, and stained with Coomassie Blue. Stained bands were excised, destained with 50% methanol in 100 mM ammonium bicarbonate, dehydrated, and digested overnight at room temperature in 100 mM ammonium bicarbonate with 50 ng sequencing-grade modified trypsin. Digestions were stopped by adding an aqueous solution of 5% formic acid, 0.2% trifluoroacetic acid (v/v) and reverse phase resin (POROS 20 R2, Perseptive Biosystems). After light shaking at 4^{o}C for 4 hours, the resin was washed with 0.5% acetic acid and bound peptides were eluted with 40% acetonitrile followed by elution with 80% acetonitrile in 0.5% acetic acid. The eluents were combined and concentrated in a speedvac. The concentrate was pressure-loaded onto a nano-HPLC column, and peptides were separated and identified as described above. The resulting spectra were searched using Sequest in the Proteome Discoverer software package (Thermo Fisher). For further validation of the Rpd3-PrA

purification, 50% of the final elution was treated as described for the Ecm5-PrA IP, with focus on excising the bands corresponding in molecular weight to Ecm5 and Snt2, and spectra were searched using X! Tandem.

Immunoprecipitations and immunoblotting

For the immunoprecipitations, strains were grown to mid-log phase and collected by centrifugation. Cells were resuspended in the Lysis Buffer described for the affinity purifications, and lysates were prepared by glass bead disruption and clarified by centrifugation. A portion of each clarified lysate was reserved for input. For Ecm5-Myc IPs, the remaining lysates were incubated with anti-cMyc beads (Sigma) for 1 hour at 4^{o}C and were washed and eluted as described for the affinity purifications. For Rpd3 IPs, lysates were incubated with either anti-Rpd3 antibody (Santa Cruz sc6655) or with goat IgG (Santa Cruz sc2028) for 1 hour at 4^{o}C, after which Protein G Dynabeads (Invitrogen) were added and allowed to incubate for another hour at 4^{o}C. Rpd3 IPs were washed as described for Ecm5-Myc IPs. The following antibodies were used for immunoblot: anti-MYC 9E10 (Millipore #05-419), anti-GFP B2 (Santa Cruz #sc9996) anti-Rpd3 (Santa Cruz #sc6655), anti-Sin3 (Santa Cruz #sc17637), and anti-beta Actin (Abcam #ab8224).

Chromatin immunoprecipitation

For the H_2O_2 ChIP-seq BY4741, Snt2-Myc, and Ecm5-Myc strains were grown to mid-log phase (OD600 = 0.4), and an aliquot of each culture was removed and fixed for ChIP. The remaining cultures were treated with H_2O_2 (final concentration 0.4 mM) for 30 minutes and then fixed similarly to the untreated samples. All samples were fixed by adding formaldehyde to a final

602 concentration of 1% and incubating at room temperature for 20 minutes with rotation. Fixation
603 was quenched by adding glycine to 125 mM final concentration. Cells were then pelleted,
604 washed 4 times in cold PBS, flash frozen, and stored at -80^{o}C.
605
606 For the Ecm5/Snt2-Myc rapamycin ChIP-seq, cultures of each strain were grown to mid-log
607 phase in SD CSM media, and an aliquot was taken and fixed as described above. Each culture
608 was then split into two cultures: one culture was treated with DMSO while the other was treated
609 with rapamycin dissolved in DMSO (50 nM final concentration). After 30 minutes these cultures
610 were fixed for ChIP as described above.
611
612 ChIP was performed essentially as described (55). Briefly, after lysing cells using 0.5 mm
613 zirconia/silica beads (Biospec Products), chromatin was sonicated using a Bioruptor sonicator to
614 150-500 bp fragments. Chromatin was incubated overnight at 4^{o}C with the Myc 9E10
615 monoclonal antibody (Millipore #05-419) and then for 2 hours with Protein G Magna ChIP
616 beads (Millipore). After washing and eluting, input and ChIP DNA samples were incubated 15
617 hours at 65^{o}C to reverse crosslinks, and then purified using Qiagen PCR purification columns per
618 manufacturer's instructions. Samples were incubated with RNase at 37^{o}C for 2 hours and then
619 purified over Qiagen columns a second time.
620
621 Sequencing libraries of input and ChIP DNAs were prepared using the Illumina TruSeq DNA kit
622 per manufacturer's instructions except that 4% of recommended DNA Adapter Index
623 concentration and 20% of the recommended PCR Primer Cocktail concentration were used per
624 library. For the final amplification step, 20 and 21 cycles of PCR were used for the H_2O_2 and

rapamycin libraries, respectively. Sequencing was performed on an Illumina HiSeq 2000, and data were analyzed following the Illumina pipeline.

Independent ChIP replicates were performed as described above and analyzed by qPCR on an Applied Biosystems StepOnePlus Real Time PCR System using Power SYBR Green PCR Master Mix (Applied Biosystems) per manufacturer's instructions. For Rpd3-Myc ChIP experiments, cells were fixed for 45 minutes at room temperature in a solution consisting of 10mM DMA and 0.25% DMSO in PBS, followed by fixation in 1% formaldehyde for 12 hours. Relative enrichment was determined by dividing the % input at the locus of interest by the % input at the right arm of telomere 6, which had low but detectable levels of enrichment for Snt2, Ecm5, and Rpd3, and served as a control for IP efficiency. Sequences of primers used for qPCR are available upon request.

RNA sequencing

BY4741, *ecm5*Δ, and *snt2*Δ cultures were treated with H_2O_2 as described for ChIP-seq experiments. RNA was isolated by hot acidic phenol extraction (56). Sequencing libraries were prepared from 4 ug total RNA using an Illumina TruSeq RNA kit per manufacturer's instructions. For the final amplification step, 15 cycles of PCR were used. An aliquot of each RNA sample was also reverse transcribed into cDNA using the Superscript III First-Strand Synthesis System (Invitrogen), and RNA-seq expression values were confirmed by qPCR. Expression qPCRs were performed as described above for ChIP-qPCRs, and expression levels of genes of interest were normalized to *ACT1* expression levels.

Sequencing Analysis

ChIP-seq reads were aligned to the sacCer2 assembly of the *S. cerevisiae* genome using the Bowtie alignment software (57). Only unique reads that mapped to a single location with no more than 2 mismatches were kept. Regions enriched for Snt2 or Ecm5 binding (i.e. peaks) were called using the MACS algorithm (58). Overlapping peaks were defined as peaks whose chromosomal coordinates overlapped by at least 200 bp, as determined using the Galaxy Server (59-61). For Snt2/Ecm5 correlation scatterplots, for each peak of either Snt2 or Ecm5 enrichment, we computed the number of Snt2 or Ecm5 reads per 1,000,000 total reads per peak size in kb (RPKM) using BedTools (62), and used the RPKM values to determine Pearson's correlation coefficients. To determine peaks where Snt2/Ecm5 enrichment increased or decreased following H_2O_2 treatment, a list of all peaks of shared Snt2/Ecm5 enrichment before or after treatment was compiled and RPKM values were calculated as described above. Peaks were then separated into those with Snt2 and Ecm5 RPKM values 1.5-fold higher, 1.5-fold lower, or unchanged following H_2O_2 treatment. Gene Ontology analysis was performed using the FuncAssociate program (31). Yeast TSS and ORF locations were obtained by querying the Ensembl database (www.ensembl.org). Promoters were defined as regions from 500 bp upstream of queried TSSs to the TSSs. The coordinates of peak summits (determined by MACS), were used to uniquely assign each peak to a promoter, ORF, or neither. To determine average Snt2/Ecm5 enrichment around yeast TSSs, a custom script was used to divide regions surrounding each TSS into 50 bp windows and count the average number of reads at all genes within those windows per million mapped reads. For motif analysis, 100-bp regions centered around peak summits were analyzed using the MEME suite (28). YEASTRACT (38) was used to search for transcription factors known to regulate Snt2/Ecm5 target genes.

RNA-seq data was aligned using the software TopHat (63), and gene expression levels and differences were calculated using the Cufflinks and Cuffdiff programs (64). All sequencing tracks were displayed using IGV (65). All ChIP-seq and RNA-seq data were submitted to the Gene Expression Omnibus (GEO; http://www.ncbi.nlm.nih.gov/geo/) database under the accession number GSE43002.

ACKNOWLEDGEMENTS

This work was supported by NIH grants CA09673 to L.A.B, GM40922 to C.D.A., and GM103314 and GM103511 to B.T.C and B.M.U., as well as by The Rockefeller University.

We thank members of the Allis Laboratory for helpful discussions, and especially Jung-Ae Kim, Kyung-Min Noh, Christina Hughes, and Laura Banaszynynski for critical reading of this manuscript. We also thank Christopher Streeter and Charles Li for helpful discussions and computational assistance.

687 REFERENCES
688
689 1. **Gasch AP, Spellman PT, Kao CM, Carmel-Harel O, Eisen MB, Storz G, Botstein D, Brown PO.** 2000. Genomic expression programs in the response of yeast cells to environmental changes. Mol Biol Cell **11:**4241-4257.
692 2. **Causton HC, Ren B, Koh SS, Harbison CT, Kanin E, Jennings EG, Lee TI, True HL, Lander ES, Young RA.** 2001. Remodeling of yeast genome expression in response to environmental changes. Mol Biol Cell **12:**323-337.
695 3. **Morano KA, Grant CM, Moye-Rowley WS.** 2012. The response to heat shock and oxidative stress in Saccharomyces cerevisiae. Genetics **190:**1157-1195.
697 4. **de Nadal E, Ammerer G, Posas F.** 2011. Controlling gene expression in response to stress. Nat Rev Genet **12:**833-845.
699 5. **Estruch F.** 2000. Stress-controlled transcription factors, stress-induced genes and stress tolerance in budding yeast. FEMS Microbiol Rev **24:**469-486.
701 6. **Harbison CT, Gordon DB, Lee TI, Rinaldi NJ, Macisaac KD, Danford TW, Hannett NM, Tagne JB, Reynolds DB, Yoo J, Jennings EG, Zeitlinger J, Pokholok DK, Kellis M, Rolfe PA, Takusagawa KT, Lander ES, Gifford DK, Fraenkel E, Young RA.** 2004. Transcriptional regulatory code of a eukaryotic genome. Nature **431:**99-104.
705 7. **Shevchenko A, Roguev A, Schaft D, Buchanan L, Habermann B, Sakalar C, Thomas H, Krogan NJ, Stewart AF.** 2008. Chromatin Central: towards the comparative proteome by accurate mapping of the yeast proteomic environment. Genome Biol **9:**R167.
709 8. **Lussier M, White AM, Sheraton J, di Paolo T, Treadwell J, Southard SB, Horenstein CI, Chen-Weiner J, Ram AF, Kapteyn JC, Roemer TW, Vo DH, Bondoc DC, Hall J, Zhong WW, Sdicu AM, Davies J, Klis FM, Robbins PW, Bussey H.** 1997. Large scale identification of genes involved in cell surface biosynthesis and architecture in Saccharomyces cerevisiae. Genetics **147:**435-450.
714 9. **Carrozza MJ, Li B, Florens L, Suganuma T, Swanson SK, Lee KK, Shia WJ, Anderson S, Yates J, Washburn MP, Workman JL.** 2005. Histone H3 methylation by Set2 directs deacetylation of coding regions by Rpd3S to suppress spurious intragenic transcription. Cell **123:**581-592.
718 10. **Keogh MC, Kurdistani SK, Morris SA, Ahn SH, Podolny V, Collins SR, Schuldiner M, Chin K, Punna T, Thompson NJ, Boone C, Emili A, Weissman JS, Hughes TR, Strahl BD, Grunstein M, Greenblatt JF, Buratowski S, Krogan NJ.** 2005. Cotranscriptional set2 methylation of histone H3 lysine 36 recruits a repressive Rpd3 complex. Cell **123:**593-605.
723 11. **Rundlett SE, Carmen AA, Kobayashi R, Bavykin S, Turner BM, Grunstein M.** 1996. HDA1 and RPD3 are members of distinct yeast histone deacetylase complexes that regulate silencing and transcription. Proc Natl Acad Sci U S A **93:**14503-14508.
726 12. **Alejandro-Osorio AL, Huebert DJ, Porcaro DT, Sonntag ME, Nillasithanukroh S, Will JL, Gasch AP.** 2009. The histone deacetylase Rpd3p is required for transient changes in genomic expression in response to stress. Genome Biol **10:**R57.
729 13. **De Nadal E, Zapater M, Alepuz PM, Sumoy L, Mas G, Posas F.** 2004. The MAPK Hog1 recruits Rpd3 histone deacetylase to activate osmoresponsive genes. Nature **427:**370-374.

14. **Kremer SB, Gross DS.** 2009. SAGA and Rpd3 chromatin modification complexes dynamically regulate heat shock gene structure and expression. J Biol Chem **284:**32914-32931.
15. **Sertil O, Vemula A, Salmon SL, Morse RH, Lowry CV.** 2007. Direct role for the Rpd3 complex in transcriptional induction of the anaerobic DAN/TIR genes in yeast. Mol Cell Biol **27:**2037-2047.
16. **Ruiz-Roig C, Vieitez C, Posas F, de Nadal E.** 2010. The Rpd3L HDAC complex is essential for the heat stress response in yeast. Mol Microbiol **76:**1049-1062.
17. **Collins SR, Miller KM, Maas NL, Roguev A, Fillingham J, Chu CS, Schuldiner M, Gebbia M, Recht J, Shales M, Ding H, Xu H, Han J, Ingvarsdottir K, Cheng B, Andrews B, Boone C, Berger SL, Hieter P, Zhang Z, Brown GW, Ingles CJ, Emili A, Allis CD, Toczyski DP, Weissman JS, Greenblatt JF, Krogan NJ.** 2007. Functional dissection of protein complexes involved in yeast chromosome biology using a genetic interaction map. Nature **446:**806-810.
18. **Cohen TJ, Lee K, Rutkowski LH, Strich R.** 2003. Ask10p mediates the oxidative stress-induced destruction of the Saccharomyces cerevisiae C-type cyclin Ume3p/Srb11p. Eukaryot Cell **2:**962-970.
19. **Page N, Sheraton J, Brown JL, Stewart RC, Bussey H.** 1996. Identification of ASK10 as a multicopy activator of Skn7p-dependent transcription of a HIS3 reporter gene. Yeast **12:**267-272.
20. **de Groot PW, Ruiz C, Vazquez de Aldana CR, Duenas E, Cid VJ, Del Rey F, Rodriquez-Pena JM, Perez P, Andel A, Caubin J, Arroyo J, Garcia JC, Gil C, Molina M, Garcia LJ, Nombela C, Klis FM.** 2001. A genomic approach for the identification and classification of genes involved in cell wall formation and its regulation in Saccharomyces cerevisiae. Comp Funct Genomics **2:**124-142.
21. **Vilella F, Herrero E, Torres J, de la Torre-Ruiz MA.** 2005. Pkc1 and the upstream elements of the cell integrity pathway in Saccharomyces cerevisiae, Rom2 and Mtl1, are required for cellular responses to oxidative stress. J Biol Chem **280:**9149-9159.
22. **Miller C, Schwalb B, Maier K, Schulz D, Dumcke S, Zacher B, Mayer A, Sydow J, Marcinowski L, Dolken L, Martin DE, Tresch A, Cramer P.** 2011. Dynamic transcriptome analysis measures rates of mRNA synthesis and decay in yeast. Mol Syst Biol **7:**458.
23. **Aitchison JD, Rout MP, Marelli M, Blobel G, Wozniak RW.** 1995. Two novel related yeast nucleoporins Nup170p and Nup157p: complementation with the vertebrate homologue Nup155p and functional interactions with the yeast nuclear pore-membrane protein Pom152p. J Cell Biol **131:**1133-1148.
24. **Molin M, Yang J, Hanzen S, Toledano MB, Labarre J, Nystrom T.** 2011. Life span extension and H(2)O(2) resistance elicited by caloric restriction require the peroxiredoxin Tsa1 in Saccharomyces cerevisiae. Mol Cell **43:**823-833.
25. **Schnell N, Krems B, Entian KD.** 1992. The PAR1 (YAP1/SNQ3) gene of Saccharomyces cerevisiae, a c-jun homologue, is involved in oxygen metabolism. Curr Genet **21:**269-273.
26. **Ahn SH, Diaz RL, Grunstein M, Allis CD.** 2006. Histone H2B deacetylation at lysine 11 is required for yeast apoptosis induced by phosphorylation of H2B at serine 10. Mol Cell **24:**211-220.
27. **Fan X, Struhl K.** 2009. Where does mediator bind in vivo? PLoS One **4:**e5029.

28. **Bailey TL, Boden M, Buske FA, Frith M, Grant CE, Clementi L, Ren J, Li WW, Noble WS.** 2009. MEME SUITE: tools for motif discovery and searching. Nucleic Acids Res **37:**W202-208.
29. **Badis G, Chan ET, van Bakel H, Pena-Castillo L, Tillo D, Tsui K, Carlson CD, Gossett AJ, Hasinoff MJ, Warren CL, Gebbia M, Talukder S, Yang A, Mnaimneh S, Terterov D, Coburn D, Li Yeo A, Yeo ZX, Clarke ND, Lieb JD, Ansari AZ, Nislow C, Hughes TR.** 2008. A library of yeast transcription factor motifs reveals a widespread function for Rsc3 in targeting nucleosome exclusion at promoters. Mol Cell **32:**878-887.
30. **Mamnun YM, Pandjaitan R, Mahe Y, Delahodde A, Kuchler K.** 2002. The yeast zinc finger regulators Pdr1p and Pdr3p control pleiotropic drug resistance (PDR) as homo- and heterodimers in vivo. Mol Microbiol **46:**1429-1440.
31. **Berriz GF, Beaver JE, Cenik C, Tasan M, Roth FP.** 2009. Next generation software for functional trend analysis. Bioinformatics **25:**3043-3044.
32. **Skulachev VP.** 1998. Cytochrome c in the apoptotic and antioxidant cascades. FEBS Lett **423:**275-280.
33. **Kuge S, Jones N, Nomoto A.** 1997. Regulation of yAP-1 nuclear localization in response to oxidative stress. Embo J **16:**1710-1720.
34. **Nevitt T, Pereira J, Rodrigues-Pousada C.** 2004. YAP4 gene expression is induced in response to several forms of stress in Saccharomyces cerevisiae. Yeast **21:**1365-1374.
35. **Herrero E, Ros J, Belli G, Cabiscol E.** 2008. Redox control and oxidative stress in yeast cells. Biochim Biophys Acta **1780:**1217-1235.
36. **Seymour IJ, Piper PW.** 1999. Stress induction of HSP30, the plasma membrane heat shock protein gene of Saccharomyces cerevisiae, appears not to use known stress-regulated transcription factors. Microbiology **145 (Pt 1):**231-239.
37. **Raitt DC, Johnson AL, Erkine AM, Makino K, Morgan B, Gross DS, Johnston LH.** 2000. The Skn7 response regulator of Saccharomyces cerevisiae interacts with Hsf1 in vivo and is required for the induction of heat shock genes by oxidative stress. Mol Biol Cell **11:**2335-2347.
38. **Abdulrehman D, Monteiro PT, Teixeira MC, Mira NP, Lourenco AB, dos Santos SC, Cabrito TR, Francisco AP, Madeira SC, Aires RS, Oliveira AL, Sa-Correia I, Freitas AT.** 2011. YEASTRACT: providing a programmatic access to curated transcriptional regulatory associations in Saccharomyces cerevisiae through a web services interface. Nucleic Acids Res **39:**D136-140.
39. **Rispail N, Di Pietro A.** 2010. The homeodomain transcription factor Ste12: Connecting fungal MAPK signalling to plant pathogenicity. Commun Integr Biol **3:**327-332.
40. **Morse RH.** 2000. RAP, RAP, open up! New wrinkles for RAP1 in yeast. Trends Genet **16:**51-53.
41. **Lieb JD, Liu X, Botstein D, Brown PO.** 2001. Promoter-specific binding of Rap1 revealed by genome-wide maps of protein-DNA association. Nat Genet **28:**327-334.
42. **Crespo JL, Hall MN.** 2002. Elucidating TOR signaling and rapamycin action: lessons from Saccharomyces cerevisiae. Microbiol Mol Biol Rev **66:**579-591, table of contents.
43. **Lee N, Erdjument-Bromage H, Tempst P, Jones RS, Zhang Y.** 2009. The H3K4 demethylase lid associates with and inhibits histone deacetylase Rpd3. Mol Cell Biol **29:**1401-1410.

44. **Hickman MJ, Winston F.** 2007. Heme levels switch the function of Hap1 of Saccharomyces cerevisiae between transcriptional activator and transcriptional repressor. Mol Cell Biol **27:**7414-7424.
45. **Weiner A, Chen HV, Liu CL, Rahat A, Klien A, Soares L, Gudipati M, Pfeffner J, Regev A, Buratowski S, Pleiss JA, Friedman N, Rando OJ.** 2012. Systematic dissection of roles for chromatin regulators in a yeast stress response. PLoS Biol **10:**e1001369.
46. **Singh RK, Gonzalez M, Kabbaj MH, Gunjan A.** 2012. Novel E3 ubiquitin ligases that regulate histone protein levels in the budding yeast Saccharomyces cerevisiae. PLoS One **7:**e36295.
47. **Breker M, Gymrek M, Schuldiner M.** 2013. A novel single-cell screening platform reveals proteome plasticity during yeast stress responses. J Cell Biol **200:**839-850.
48. **Longtine MS, McKenzie A, 3rd, Demarini DJ, Shah NG, Wach A, Brachat A, Philippsen P, Pringle JR.** 1998. Additional modules for versatile and economical PCR-based gene deletion and modification in Saccharomyces cerevisiae. Yeast **14:**953-961.
49. **Oeffinger M, Wei KE, Rogers R, DeGrasse JA, Chait BT, Aitchison JD, Rout MP.** 2007. Comprehensive analysis of diverse ribonucleoprotein complexes. Nat Methods **4:**951-956.
50. **Cristea IM, Chait BT.** 2011. Conjugation of magnetic beads for immunopurification of protein complexes. Cold Spring Harb Protoc **2011:**pdb prot5610.
51. **Cristea IM, Chait BT.** 2011. Affinity purification of protein complexes. Cold Spring Harb Protoc **2011:**pdb prot5611.
52. **Craig R, Beavis RC.** 2004. TANDEM: matching proteins with tandem mass spectra. Bioinformatics **20:**1466-1467.
53. **Gavin AC, Bosche M, Krause R, Grandi P, Marzioch M, Bauer A, Schultz J, Rick JM, Michon AM, Cruciat CM, Remor M, Hofert C, Schelder M, Brajenovic M, Ruffner H, Merino A, Klein K, Hudak M, Dickson D, Rudi T, Gnau V, Bauch A, Bastuck S, Huhse B, Leutwein C, Heurtier MA, Copley RR, Edelmann A, Querfurth E, Rybin V, Drewes G, Raida M, Bouwmeester T, Bork P, Seraphin B, Kuster B, Neubauer G, Superti-Furga G.** 2002. Functional organization of the yeast proteome by systematic analysis of protein complexes. Nature **415:**141-147.
54. **Ghaemmaghami S, Huh WK, Bower K, Howson RW, Belle A, Dephoure N, O'Shea EK, Weissman JS.** 2003. Global analysis of protein expression in yeast. Nature **425:**737-741.
55. **Aparicio O, Geisberg JV, Sekinger E, Yang A, Moqtaderi Z, Struhl K.** 2005. Chromatin immunoprecipitation for determining the association of proteins with specific genomic sequences in vivo. Curr Protoc Mol Biol **Chapter 21:**Unit 21 23.
56. **Collart MA, Oliviero S.** 2001. Preparation of yeast RNA. Curr Protoc Mol Biol **Chapter 13:**Unit13 12.
57. **Langmead B, Trapnell C, Pop M, Salzberg SL.** 2009. Ultrafast and memory-efficient alignment of short DNA sequences to the human genome. Genome Biol **10:**R25.
58. **Zhang Y, Liu T, Meyer CA, Eeckhoute J, Johnson DS, Bernstein BE, Nusbaum C, Myers RM, Brown M, Li W, Liu XS.** 2008. Model-based analysis of ChIP-Seq (MACS). Genome Biol **9:**R137.

59. **Goecks J, Nekrutenko A, Taylor J.** 2010. Galaxy: a comprehensive approach for supporting accessible, reproducible, and transparent computational research in the life sciences. Genome Biol **11:**R86.
60. **Blankenberg D, Von Kuster G, Coraor N, Ananda G, Lazarus R, Mangan M, Nekrutenko A, Taylor J.** 2010. Galaxy: a web-based genome analysis tool for experimentalists. Curr Protoc Mol Biol **Chapter 19:**Unit 19 10 11-21.
61. **Giardine B, Riemer C, Hardison RC, Burhans R, Elnitski L, Shah P, Zhang Y, Blankenberg D, Albert I, Taylor J, Miller W, Kent WJ, Nekrutenko A.** 2005. Galaxy: a platform for interactive large-scale genome analysis. Genome Res **15:**1451-1455.
62. **Quinlan AR, Hall IM.** 2010. BEDTools: a flexible suite of utilities for comparing genomic features. Bioinformatics **26:**841-842.
63. **Trapnell C, Pachter L, Salzberg SL.** 2009. TopHat: discovering splice junctions with RNA-Seq. Bioinformatics **25:**1105-1111.
64. **Trapnell C, Williams BA, Pertea G, Mortazavi A, Kwan G, van Baren MJ, Salzberg SL, Wold BJ, Pachter L.** 2010. Transcript assembly and quantification by RNA-Seq reveals unannotated transcripts and isoform switching during cell differentiation. Nat Biotechnol **28:**511-515.
65. **Robinson JT, Thorvaldsdottir H, Winckler W, Guttman M, Lander ES, Getz G, Mesirov JP.** 2011. Integrative genomics viewer. Nat Biotechnol **29:**24-26.

889 **FIGURE LEGENDS**

890 **FIG 1. Snt2 associates with Ecm5 and the Rpd3 deacetylase.** (A) Domain structures of Snt2,
891 Ecm5, and Rpd3. BAH: Bromo-Adjacent Homology; PHD: Plant Homeodomain Finger; SANT:
892 Spt3-Ada3-N'CoR-TFIIS; ARID: AT Rich Interaction Domain; JmjC: Jumonji C; HDAC:
893 histone deacetylase. (B) Silver-stained SDS-PAGE gel of eluates from Snt2-PrA and control (no
894 tag) affinity-purifications. Proteins identified by LC-MS are listed next to bands of the
895 appropriate size. Rpd3 comigrated on the gel with IgG. (C) Coomassie-stained gel analysis of
896 Ecm5-PrA and control purifications. Proteins identified by LC-MS are listed next to the
897 corresponding bands. (D) Lysates of untagged, Ecm5-Myc, Snt2-GFP, or Ecm5-Myc Snt2-GFP
898 strains were immunoprecipitated with anti-Myc antibody, and inputs and IPs were
899 immunoblotted (IB) with anti-Myc (to detect Ecm5), anti-GFP (to detect Snt2), anti-Rpd3, or
900 anti-Sin3.

901

902 **FIG 2. Cells lacking Snt2 or Rpd3 are resistant to H_2O_2.** (A) Five-fold serial dilutions of
903 wild-type (WT) or indicated knockout strains were spotted onto YPD plates that were untreated
904 or supplemented with 2.3 mM H_2O_2. Plates were imaged after 2 days. (B) Log-phase cultures of
905 wild-type or indicated knockout strains were treated with 0.4 mM H_2O_2 for 4 hours. Percent
906 survival was determined by CFU assay. Data are means and SEMs from 3 biological replicates.
907 ** denotes $p<0.01$ (C and D) Plate spotting assays with the indicated knockout strains were
908 performed as in (A).

909

910 **FIG 3. H_2O_2 treatment does not affect the levels of Snt2 and Rpd3 associating with Ecm5,**
911 **or the levels of Ecm5 and Snt2 associating with Rpd3.** (A) Immunoblot analysis of Myc

912 immunoprecipitations from *ECM5-MYC SNT2-GFP* or *SNT2-GFP* strains that were untreated or
913 treated with H_2O_2. For Ecm5-Myc and Snt2-GFP immunoblots, input is 15% of IP; for Rpd3
914 immunoblot, input is 1% of IP. (B) Immunoblot analysis of Rpd3 immunoprecipitation from the
915 *ECM5-MYC SNT2-GFP* strain treated as in (A). Inputs are 15% of IPs.
916
917 **FIG 4. Snt2 and Ecm5 are highly colocalized and associate with additional promoters after**
918 **H_2O_2 stress.** (A) ChIP-seq tracks showing Snt2 and Ecm5 ChIP enrichment in a representative
919 region before and after H_2O_2 treatment. The coverage values for each track are scaled by
920 1,000,000 / the number of reads, and the scale of the y axes for all tracks is shown in brackets.
921 The locations of genes and peaks, and the chromosomal coordinates are shown under the tracks.
922 (B) Venn diagrams show the majority of Snt2 and Ecm5 ChIP peaks overlap. (C) Correlations
923 between Snt2 and Ecm5 enrichment before and after H_2O_2 treatment (Pearson's correlation
924 coefficients indicated). (D) The genomic distributions of shared Snt2/Ecm5 peaks before and
925 after H_2O_2 stress. (E) The average number of Snt2 (left panel) or Ecm5 (right panel) ChIP-seq
926 reads per 50 bp window around transcription start sites (TSSs) for all yeast genes, scaled by
927 1,000,000/total reads. (F) Overlaps of Snt2 (top) or Ecm5 (bottom) peaks before and after H_2O_2
928 treatment. (G) Box-whisker plots showing the distributions of Snt2 and Ecm5 enrichment at all
929 peak regions in the treated and untreated datasets. p-values determined by Wilcoxon rank sum
930 test. (H) Snt2 (top) or Ecm5 (bottom) enrichment levels at peaks after H_2O_2 treatment, relative to
931 levels before treatment. Peaks where Snt2/Ecm5 enrichment was >1.5-fold increased, >1.5-fold
932 decreased, or unchanged after treatment are colored purple, orange, or gray, respectively. (I)
933 Motif analysis using the 20 most-enriched Snt2/Ecm5 peaks (left) or all peaks where Snt2/Ecm5
934 levels increased after treatment (right). (J) Categories of genes significantly enriched by GO

analysis of Snt2/Ecm5 peaks that increased, decreased, or did not change enrichment after treatment.

FIG 5. After H_2O_2 treatment, Snt2 and Ecm5 localize to stress and metabolism genes. (A) Examples of ESR genes whose promoters are enriched for Snt2 and Ecm5 after H_2O_2 treatment. For bidirectional promoters, the gene associated with the category above the panels is in larger font. (B) ChIP-seq results were confirmed by ChIP-qPCR. Relative enrichment was determined by normalizing % inputs at the target locus to % inputs at a control region on the right arm of telomere 6. Means and SEMs of 3 biological replicates are shown. Samples in which the ChIP enrichment after treatment differ significantly from enrichment before treatment are indicated with * ($p<0.05$) or ** ($p<0.01$). Enrichment in the *ACT1* ORF is shown as a negative control.

FIG 6. Snt2 and Ecm5 are required for Rpd3 recruitment to super-enriched promoters, but not for recruitment of the Rpd3(L) complex member Sds3. (A) Promoters super-enriched for Snt2 and Ecm5 (note bracketed scales for ChIP-seq tracks) before and after H_2O_2 treatment. (B) ChIP-qPCR confirmation of high levels of Snt2 and Ecm5 at super-enriched promoters shown in (A). Data were normalized as in (5B). (C) Control immunoblots showing that deletion of *SNT2* or *ECM5* did not affect Rpd3-Myc levels, and that deletion of *SNT2* did not affect Sds3-Myc levels, before or after H_2O_2 treatment. Actin blots serve as a loading controls. (D) Rpd3-Myc ChIP-qPCR performed on untagged, *RPD3-MYC*, *RPD3-MYC snt2*Δ, or *RPD3-MYC ecm5*Δ strains that were treated with H_2O_2. Data were normalized as in (5B). (E) Sds3-Myc ChIP-qPCR performed on untagged, *SDS3-MYC*, or *SDS3-*

*MYC snt2*Δ strains that were treated with H_2O_2. Data show mean and standard deviations of 3 independent measurements, and are representative of 2 experiments.

FIG 7. Snt2 is required for proper expression of ChIP target genes after H_2O_2 treatment. (A) Numbers of genes significantly up- or down-regulated from wild-type (WT) levels in the *snt2*Δ or *ecm5*Δ strains, before and after H_2O_2 treatment. (B) Two cell wall genes mis-expressed in opposite ways in the *snt2*Δ and *ecm5*Δ strains: graphs show $\log_2$ ratios of expression in the mutant strains relative to WT levels before treatment. (C) Categories of genes significantly up- or down-regulated in the *snt2*Δ strain relative to wild-type levels after H_2O_2 treatment. (D) Overlap between Snt2/Ecm5 H_2O_2-enriched target genes that were up- or down-regulated relative to WT in the *snt2*Δ strain after treatment, and target genes that changed expression in the WT strain after treatment. (E) Target genes that function in either the oxidative stress response or the cytochrome *c* pathway that were up- or down-regulated in the *snt2*Δ strain after treatment. Graphs show $\log_2$ ratios of expression levels in *snt2*Δ after treatment relative to WT after treatment. (F) Heatmap showing expression levels of the 309 genes described in (D). Four clusters of genes with similar expression patterns are noted at top of panel. (G) Scatterplots of the 309 genes described in (D), comparing the $\log_2$ expression ratios in *snt2*Δ cells after treatment relative to WT levels after treatment (y axis) to the $\log_2$ expression ratios in WT cells after treatment relative to WT levels before treatment (x axis). In right 3 panels, genes in the categories above the plots are colored red. (H) Overlap between 309 genes and Ste12 (left) or Rap1 (right) target genes.

FIG 8. Rapamycin treatment recapitulates a subset of the Snt2 and Ecm5 localization changes seen after H_2O_2 treatment.

(A) Serial dilutions of the indicated WT or knockout strains were spotted onto SD-CSM plates supplemented with DMSO alone or rapamycin dissolved in DMSO (50 nM final conc). (B) Snt2/Ecm5 ChIP-seq enrichment in control and rapamycin-treated cells at a representative region on chromosome VII. Arrows mark regions where Snt2 and Ecm5 levels were enriched after rapamycin treatment. (C) Overlap between peaks where levels of Snt2 and Ecm5 levels were at least 1.5-fold higher after rapamycin treatment and peaks where Snt2/Ecm5 levels were higher after H_2O_2 treatment. (D) Promoters enriched for Snt2 and Ecm5 after H_2O_2 or rapamycin treatment.

TABLE 1 Yeast strains used in this study[a]

Strain	Genotype	Source
BY4741	*MATa his3Δ1 leu2Δ0 met15Δ0 ura3Δ0*	Open Biosystems
LBY101	*MATa ECM5-PrA::HIS5*	This study
LBY102	*MATa SNT2-PrA::HIS5*	This study
LBY103	*MATa RPD3-PrA::HIS5*	This study
LBY104	*MATa ECM5-13MYC::KAN*	This study
LBY105	*MATa SNT2-13MYC::KAN*	This study
LBY106	*MATa SNT2-GFP::NAT*	This study
LBY107	*MATa ECM5-13MYC::KAN SNT2-GFP::NAT*	This study
LBY108	*MATa ecm5Δ::KAN*	Open Biosystems
LBY109	*MATa snt2Δ::KAN*	Open Biosystems
LBY110	*MATa rpd3Δ::KAN*	This study
LBY111	*MATa yap1Δ::KAN*	Open Biosystems
LBY112	*MATa gpr1Δ::KAN*	Open Biosystems
LBY113	*MATa sin3Δ::KAN*	Open Biosystems
LBY114	*MATa sap30Δ::KAN*	Open Biosystems
LBY115	*MATa cti6Δ::KAN*	Open Biosystems
LBY116	*MATa snt2Δ::KAN ecm5Δ::HYG*	This study
LBY117	*MATa snt2Δ::KAN rpd3Δ::HYG*	This study
LBY118	*MATa rpd3Δ::KAN ecm5Δ::HYG*	This study
LBY119	*MATa RPD3-13MYC::KAN*	This study
LBY120	*MATa RPD3-13MYC::KAN snt2Δ::HYG*	This study
LBY121	*MATa RPD3-13MYC::KAN ecm5Δ::HYG*	This study
LBY122	*MATa SDS3-13MYC::KAN*	This study
LBY123	*MATa SDS3-13MYC::KAN snt2Δ::HYG*	This study

[a]All strains isogenic to BY4741

993
994

TABLE 2 Peptides identified co-purifying with Snt2-PrA[a]

Protein	log(e)	% protein coverage	unique peptides	total peptides	phos sites[b]
Ecm5	-560.0	34	44	69	
Snt2	-340.9	21	30	38	S641
Rpd3	-108.2	26	9	15	
Rps21b[c]	-53.2	56	5	7	
Rpp2b[c]	-46.8	50	4	4	
Rpl19b[c]	-40.7	22	4	4	
Rps6b[c]	-35.3	15	3	3	
Rpp2a[c]	-34.0	32	3	3	
Rpl18b[c]	-27.0	17	3	3	

[a] Proteins also identified in control purification or known to be contaminants of PrA purifications (7, 53) were omitted.

[b] Phosphorylated peptide confirmed by MS-MS.

[c] While not previously reported as contaminants, these proteins are highly abundant (54) and are therefore likely contaminants.

1001 **TABLE 3** Genes whose promoters were super enriched for Snt2 and Ecm5

Peak	Gene	Function
1	*CYC3*	cytochrome *c* heme lyase
	CDC19	pyruvate kinase
2	*SSA3*	HSP70-family chaperone involved in the stress response
3	*POT1*	thiolase involved in beta-oxidation of fatty acids
	BNR1	formin involved in actin polymerization
4	*PGU1*	secreted polygalacturonase used to hydrolyze plant pectins
5	*STM1*	ribosome-binding protein required for translation under nutrient stress
	YLR149C	unknown
6	*IPI3*	component of Rix1 complex involved in rRNA processing
	YNL181W	putative oxidoreductase
7	*MSN1*	transcriptional activator involved in the stress response
8	*CUP9*	transcriptional repressor of *PTR2* peptide transporter gene
9	*CUR1*	protein sorting factor induced in stressed cells
10	*GDB1*	glycogen debranching enzyme involved in glycogen degradation

1002

FIG 1

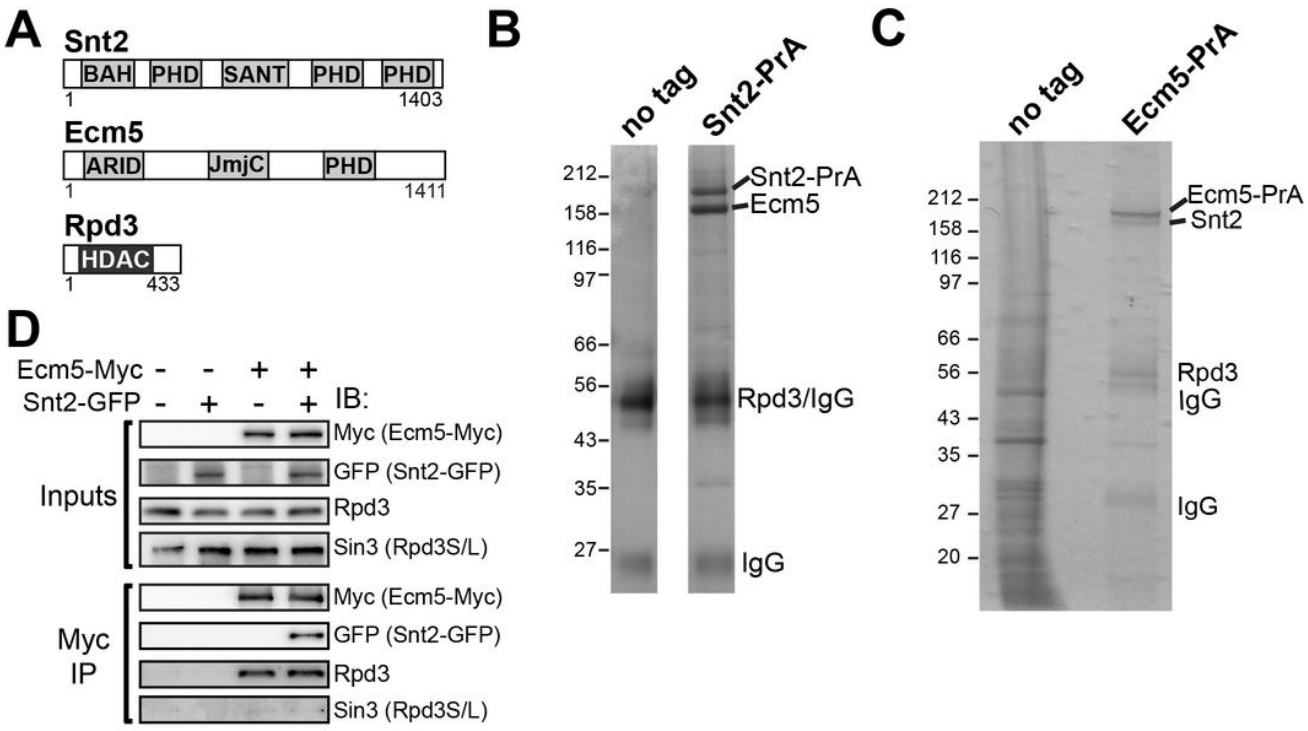

FIG 1. Snt2 associates with Ecm5 and the Rpd3 deacetylase.
(A) Domain structures of Snt2, Ecm5, and Rpd3. BAH: Bromo-Adjacent Homology; PHD: Plant Homeodomain Finger; SANT: Spt3-Ada3-N'CoR-TFIIS; ARID: AT Rich Interaction Domain; JmjC: Jumonji C; HDAC: histone deacetylase. (B) Silver-stained SDS-PAGE gel of eluates from Snt2-PrA and control (no tag) affinity-purifications. Proteins identified by LC-MS are listed next to bands of the appropriate size. Rpd3 comigrated on the gel with IgG. (C) Coomassie-stained gel analysis of Ecm5-PrA and control purifications. Proteins identified by LC-MS are listed next to the corresponding bands. (D) Lysates of untagged, Ecm5-Myc, Snt2-GFP, or Ecm5-Myc Snt2-GFP strains were immunoprecipitated with anti-Myc antibody, and inputs and IPs were immunoblotted (IB) with anti-Myc (to detect Ecm5), anti-GFP (to detect Snt2), anti-Rpd3, or anti-Sin3.

FIG 2

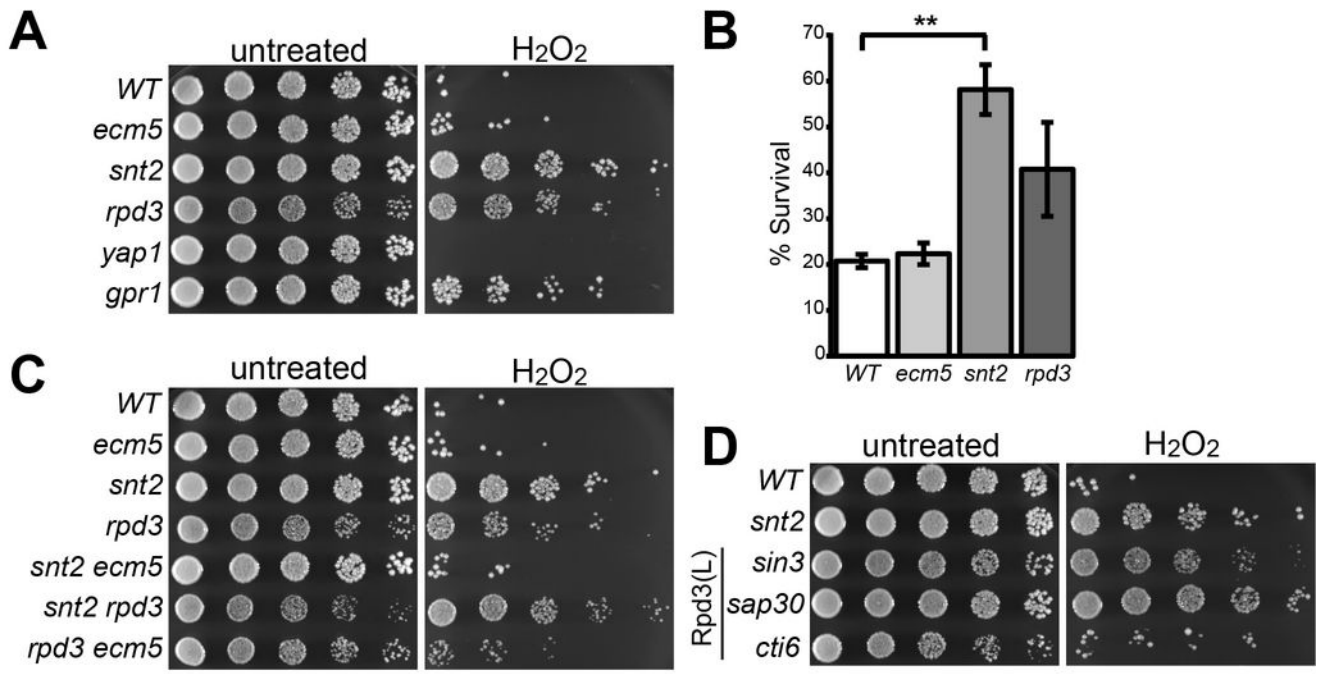

FIG 2. Cells lacking Snt2 or Rpd3 are resistant to H_2O_2.
(A) Five-fold serial dilutions of wild-type (WT) or indicated knockout strains were spotted onto YPD plates that were untreated or supplemented with 2.3 mM H_2O_2. Plates were imaged after 2 days. (B) Log-phase cultures of wild-type or indicated knockout strains were treated with 0.4 mM H_2O_2 for 4 hours. Percent survival was determined by CFU assay. Data are means and SEMs from 3 biological replicates. ** denotes $p<0.01$ (C and D) Plate spotting assays with the indicated knockout strains were performed as in (A).

FIG 3

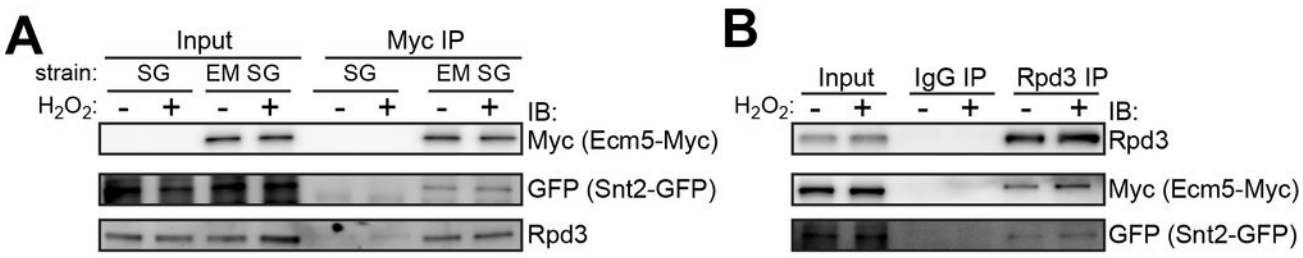

FIG 3. H_2O_2 treatment does not affect the levels of Snt2 and Rpd3 associating with Ecm5, or the levels of Ecm5 and Snt2 associating with Rpd3.
(A) Immunoblot analysis of Myc immunoprecipitations from the *ECM5-MYC SNT2-GFP* or *SNT2-GFP* strains that were untreated or treated with H_2O_2. For Ecm5-Myc and Snt2-GFP immunoblots, input is 15% of IP; for Rpd3 immunoblot, input is 1% of IP. (B) Immunoblot analysis of Rpd3 immunoprecipitation from the *ECM5-MYC SNT2-GFP* strain treated as in (A). Inputs are 15% of IPs.

FIG 4

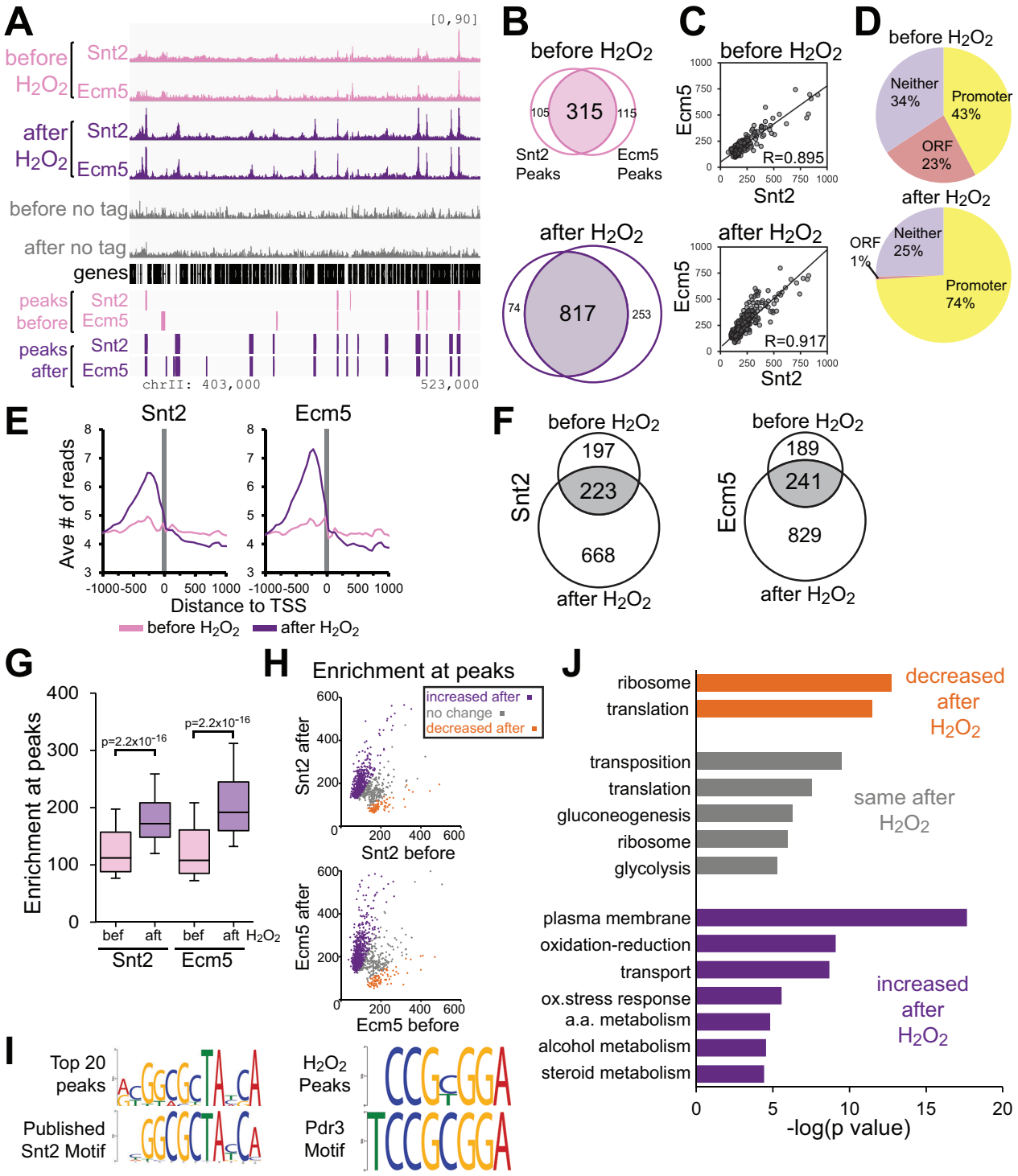

FIG 4. Snt2 and Ecm5 are highly colocalized and associate with additional promoters after H_2O_2 stress.
(A) ChIP-seq tracks showing Snt2 and Ecm5 ChIP enrichment in a representative region before and after H_2O_2 treatment. The coverage values for each track are scaled by 1,000,000 / the number of reads, and the scale of the y axes for all tracks is shown in brackets. The locations of genes and peaks, and the chromosomal coordinates are shown under the tracks. (B) Venn diagrams show the majority of Snt2 and Ecm5 ChIP peaks overlap. (C) Correlations between Snt2 and Ecm5 enrichment before and after H_2O_2 treatment (Pearson's correlation coefficients indicated). (D) The genomic distribution of shared Snt2/Ecm5 peaks before and after H_2O_2 stress. (E) The average number of Snt2 (left panel) or Ecm5 (right panel) ChIP-seq reads per 50 bp window around transcription start sites (TSSs) for all yeast genes, scaled by 1,000,000/total reads. (F) Overlaps of Snt2 (top) or Ecm5 (bottom) peaks before and after H_2O_2 treatment. (G) Box-whisker plots showing the distributions of Snt2 and Ecm5 enrichment at all peak regions in the treated and untreated datasets. p-values determined by Wilcoxon rank sum test. (H) Snt2 (top) or Ecm5 (bottom) enrichment levels at peaks after H_2O_2 treatment, relative to levels before treatment. Peaks where Snt2/Ecm5 enrichment was >1.5-fold increased, >1.5-fold decreased, or unchanged after treatment are colored purple, orange, or gray, respectively. (I) Motif analyis using the 20 most-enriched Snt2/Ecm5 peaks (left) or all peaks where Snt2/Ecm5 levels increased after treatment (right). (J) Categories of genes significantly enriched by GO analysis of Snt2/Ecm5 peaks that increased, decreased, or did not change enrichment after treatment.

FIG 5

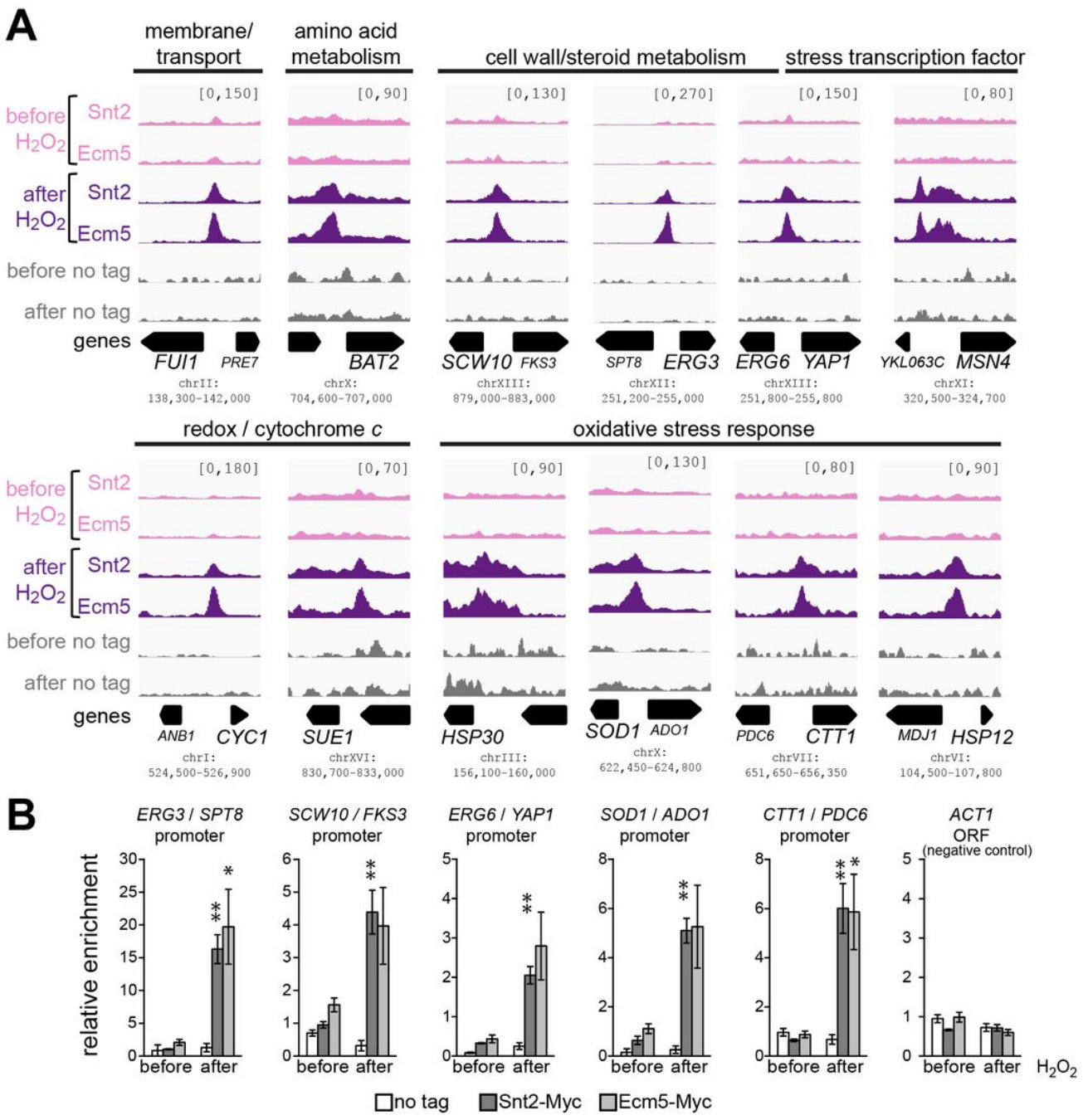

FIG 5. After H_2O_2 treatment Snt2 and Ecm5 localize to stress and metabolism gene promoters. (A) Examples of ESR genes whose promoters are enriched for Snt2 and Ecm5 after H_2O_2 treatment. For bidirectional promoters, the gene associated with the category above the panels is in larger font. (B) ChIP-seq results were confirmed by ChIP-qPCR. Relative enrichment was determined by normalizing % inputs at the target locus to % inputs at a control region on the right arm of telomere 6. Means and SEMs of 3 biological replicates are shown. Samples in which the ChIP enrichment after treatment differ significantly from enrichment before treatment are indicated with * ($p<0.05$) or ** ($p<0.01$). Enrichment in the *ACT1* ORF is shown as a negative control.

FIG 6

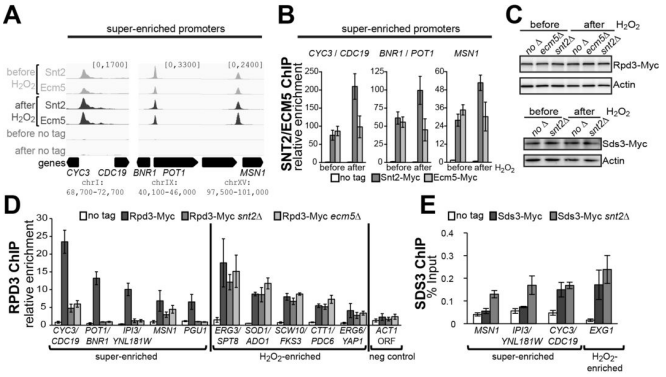

FIG 6. Snt2 and Ecm5 are required for Rpd3 recruitment to super enriched promoters, but not for recruitment of the Rpd3(L) complex member Sds3.
(A) Promoters super-enriched for Snt2 and Ecm5 (note bracketed scales for ChIP-seq tracks) before and after H_2O_2 treatment. (B) ChIP-qPCR confirmation of high levels of Snt2 and Ecm5 at super-enriched promoters shown in (A). Data were normalized as in (5B). (C) Control immunoblots showing that deletion of *SNT2* or *ECM5* did not affect Rpd3-Myc levels, and that deletion of *SNT2* did not affect Sds3-Myc levels, before or after H_2O_2 treatment. Actin blots serve as a loading controls. (D) Rpd3-Myc ChIP-qPCR performed on untagged, *RPD3-MYC*, *RPD3-MYC snt2*Δ, or *RPD3-MYC ecm5*Δ strains that were H_2O_2-treated. Data were normalized as in (5B). (E) Sds3-Myc ChIP-qPCR performed on untagged, *SDS3-MYC*, or *SDS3-MYC snt2*Δ strains that were H_2O_2-treated. Data show mean and standard deviations of 3 independent measurements, and are representative of 2 experiments.

FIG 7

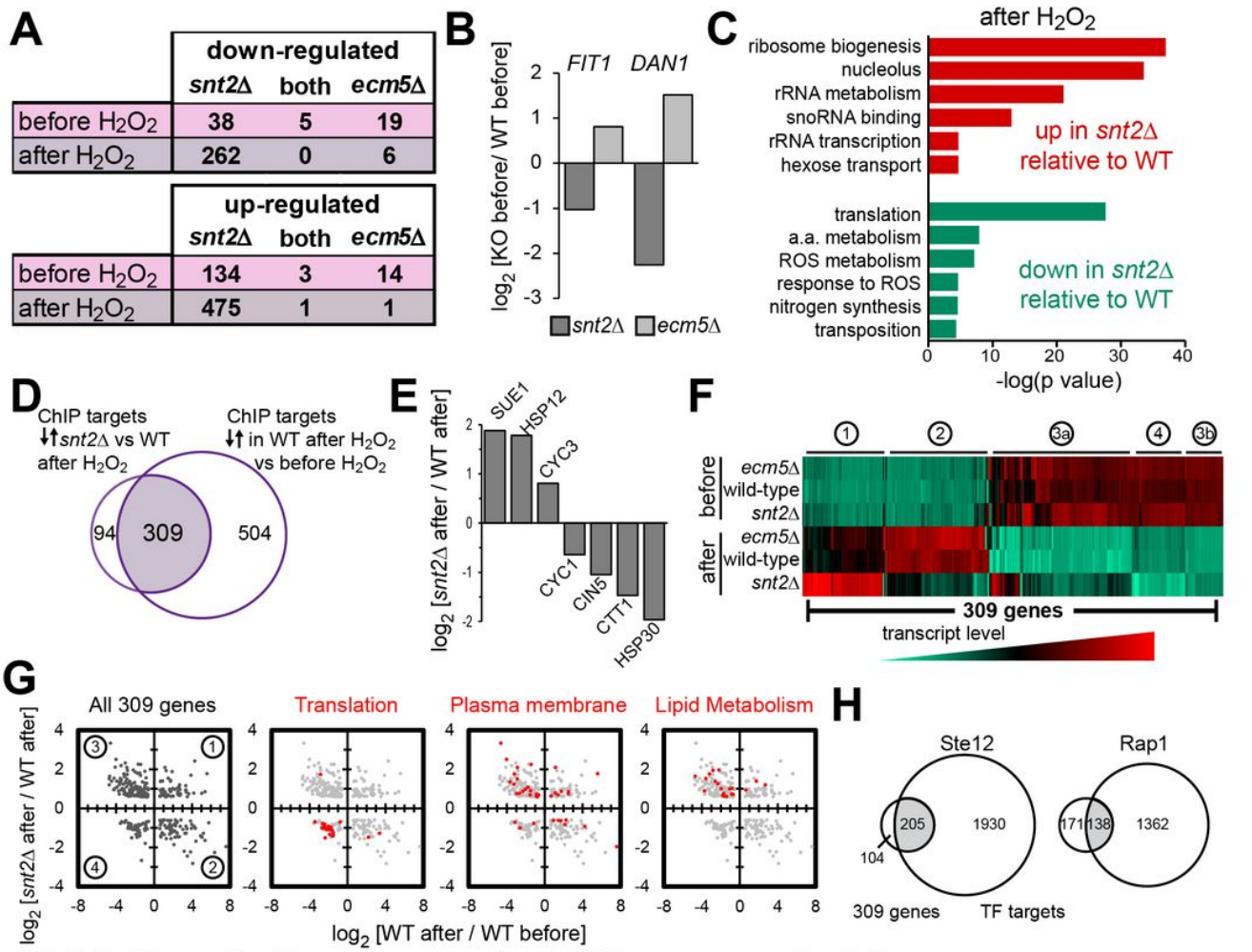

FIG 7. Snt2 is required for proper expression of ChIP target genes after H_2O_2 treatment.
(A) Numbers of genes significantly up- or down-regulated from wild-type (WT) levels in the *snt2*Δ or *ecm5*Δ strains, before and after H_2O_2 treatment. (B) Two cell wall genes mis-expressed in opposite ways in the *snt2*Δ and *ecm5*Δ strains: graphs show $\log_2$ ratios of expression in the mutant strains relative to WT levels before treatment. (C) Categories of genes significantly up- or down-regulated in the *snt2*Δ strain relative to WT levels after treatment. (D) Overlap between Snt2/Ecm5 H_2O_2-enriched target genes that were up- or down-regulated relative to WT in the *snt2*Δ strain after treatment relative to WT levels after treatment, and target genes that changed expression in the WT strain after treatment. (E) Examples of target genes that function in either the oxidative stress response or the cytochrome *c* pathway whose expression differed between the *snt2*Δ and WT strains after treatment. Graphs show $\log_2$ ratios of expression levels in *snt2*Δ after treatment relative to WT after treatment. (F) Heatmap showing expression levels of the 309 genes described in (D). Four clusters of genes with similar expression patterns are noted at top of panel. (G) Scatterplots of the 309 genes described in (D), comparing the $\log_2$ expression ratios in *snt2*Δ cells after treatment relative to WT levels after treatment (y axis) to the $\log_2$ expression ratios in WT cells after treatment relative to WT levels before treatment (x axis). In right 3 panels, genes in the categories above the plots are colored red. (H) Overlap between 309 genes and Ste12 (left) or Rap1 (right) target genes.

FIG 8

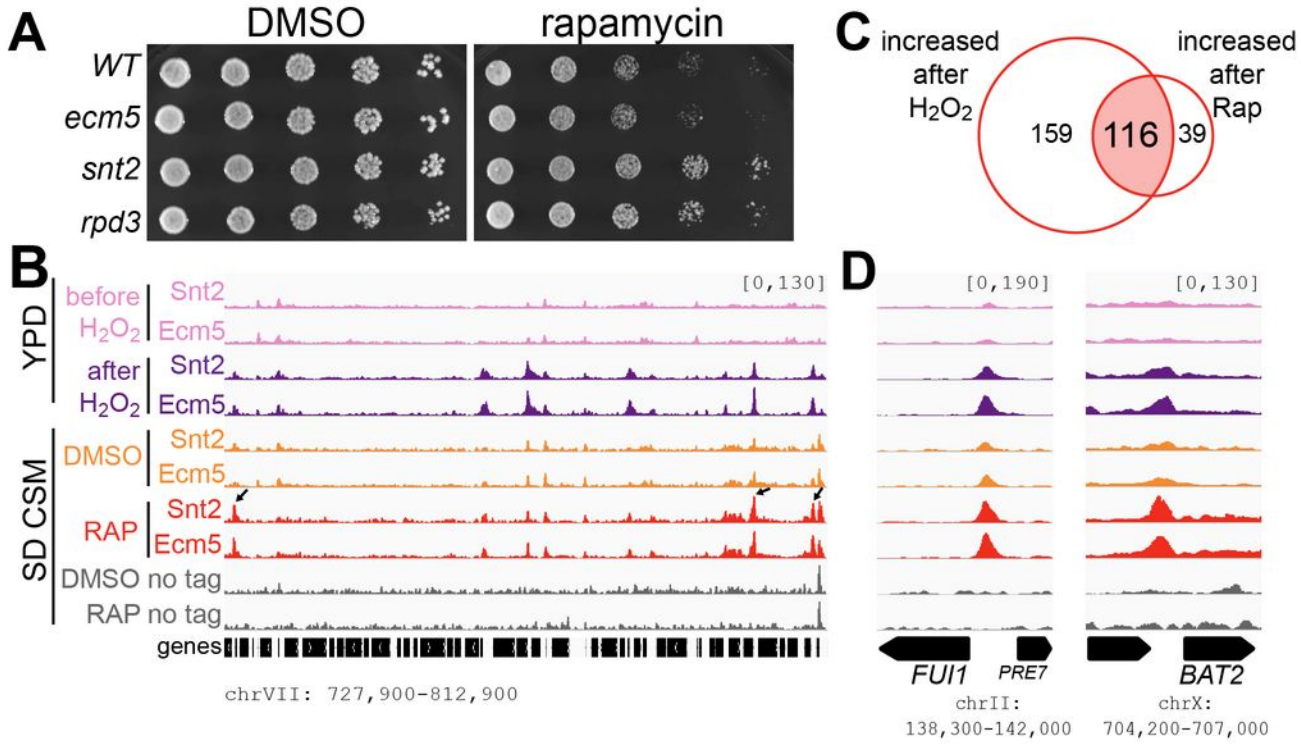

FIG 8. Rapamycin treatment recapitulates a subset of the Snt2 and Ecm5 localization changes seen after H_2O_2 treatment.
(A) Serial dilutions of the indicated WT or knockout strains were spotted onto SD-CSM plates supplemented with DMSO alone or rapamycin dissolved in DMSO (50 nM final conc). (B) Snt2/Ecm5 ChIP-seq enrichment in control and rapamycin-treated cells, at a representative region along chromosome VII. Arrows mark regions where Snt2 and Ecm5 levels were enriched after rapamycin treatment. (C) Overlap between peaks where Snt2 and Ecm5 levels were at least 1.5-fold higher after rapamycin treatment and peaks where Snt2/Ecm5 levels were higher after H_2O_2 treatment. (D) Promoters enriched for Snt2 and Ecm5 after H_2O_2 or rapamycin treatment.